Creation of Coherent Complex Pressure Measurements Through Overlapping Scan-Based Measurements

Jazmin S. Myres

A senior thesis submitted to the faculty of
Brigham Young University
in partial fulfillment of the requirements for the degree of

Bachelor of Science

Kent Gee, Tracianne Neilsen, Advisors

Department of Physics and Astronomy
Brigham Young University
April 2014

ABSTRACT

Creation of Coherent Complex Pressure Measurements Through

Overlapping Scan-Based Measurements

Jazmin S. Myres

Department of Physics and Astronomy

Bachelor of Science

In scan-based array measurements, stationary reference sensors are needed to temporally correlate the different measurement scans and produce coherent complex pressure fields that can be used to perform near-field acoustical holography (NAH). Because the number of references required increases with the number of subsources contributing to the sound field, an extended, partially correlated source (e.g., a turbulent jet) comprising many ill-defined sources can result in significantly increased measurement complexity and expense. Demonstrated here a is a new approach to creating spatiotemporally coherent pressures using self-referencing between overlapping measurement positions instead of separate reference channels. A laboratory experiment was designed and the data have been used to explore "stitching" together a complex pressure field. This experiment is described and the “stitching” method is detailed. To successfully execute the technique, unwrapping of intrascan phases is first accomplished with a two-dimensional phase unwrapping algorithm. Individual scan positions are then stitched together using median phase differences between multiple adjacent scans to create coherent planes of data. Amplitude-stitching is done by averaging across scans and preserving the integrated squared pressure across the overall aperture. The validity of this method is shown by showing that a consistent local coherence maintained through the stitching process. The technique is applied to jet noise, and the possibility of applying it to NAH is discussed. This technique provides direction for efficient experimental design for scan-based array measurements of extended sources.

Contents

Chapter 1: Introduction

1.1 Jet Noise and Near-Field Acoustical Holography

This thesis presents a new method of creating coherent complex pressure fields for use in performing near-field acoustical holography to characterize and understand jet noise, with the ultimate goal of reducing the hearing loss attributed to military jet engines. While tactical aircraft play a critical role in the success of current military operations, they present a danger to the hearing of personnel working in and around aircraft in the extreme sonic environment resulting from "jet noise."

Jet noise is understood to be the result of fluid turbulence in the large superheated supersonic exhaust plume extending out of a jet engine.[1] [2] This fluid turbulence has small and large components contributing to the uncorrelated and correlated components of jet noise, which is best described as a partially correlated source.[3] [4] Understanding this complicated, large, and partially coherent source is the key to developing and implementing strategies to reduce hearing loss among military personnel.

Near-field acoustical holography (NAH) is a vital tool in source characterization of jet noise that allows researchers to remotely interrogate the source. When researching a turbulent, heated, extended fluid source such as jet noise, measurements cannot be taken at the source without interfering with the jet flow. Additionally, typical acoustical measurement transducers cannot withstand the extreme environment presented by a military jet engine. To circumvent these challenges and infer source conditions and characteristics, NAH is performed using planes of data taken at a safe distance from the source, and the sound field is inversely projected to the near-field source region.[5] Using NAH allows researchers to better understand the source of jet noise; however, applying NAH to a jet source provides unique computational challenges.

Pioneers of near-field acoustical holography have refined the process to allow for many source geometries and measurement conditions. Acoustical holography can be performed on planar[6], spherical, cylindrical[7], and conical projections using straight forward methods.[8] Only recently, through the work of Wall *et al.*, has NAH been applied specifically to military jet noise.[9] [10] In order for NAH to be effective on a complicated source such as jet noise, there are many measurement requirements that must be met.

The source and measurement requirements for performing near-field acoustical holography are as follows. The source must be partially coherent to the extent that there is a strong correlation between adjacent microphone positions. The spatial sampling must be dense enough that there are at least two measurement positions per wavelength. The measurement plane must be far enough from the source that free-field acoustic conditions exist, and it must be large enough to adequately cover the source aperture. Lastly, the entire measurement plane must be temporally correlated. These requirements result in a large, in phase, array of complex acoustic pressures that completely cover the source aperture at a safe distance from the source region.[11]

1.2 Complex Pressure Plane

To obtain a complex pressure plane for use in NAH, measurements are either taken simultaneously by a large stationary array, or in smaller scans that need to be temporally correlated post-measurement. Diagrams of a stationary array measurement and a scan-based measurement with reference microphones are shown in Figure 1 part a) and b). These methods both provide a large plane of in-phase measurements that can be used to generate the complex pressures necessary to perform NAH, and have been successfully used in the past.[12] For an extended source requiring a large measurement plane, the scan-by-

scan method is most cost effective. For example, a 25 m source region (such as that produced by a military jet plume) requires upwards of 2000 measurement positions to achieve an adequate spatial density; this can only reasonably be obtained using a much smaller scanning array. Traditionally, temporal correlation of individual measurement scans has been performed using data from stationary reference microphones (Figure 1 part (b)).

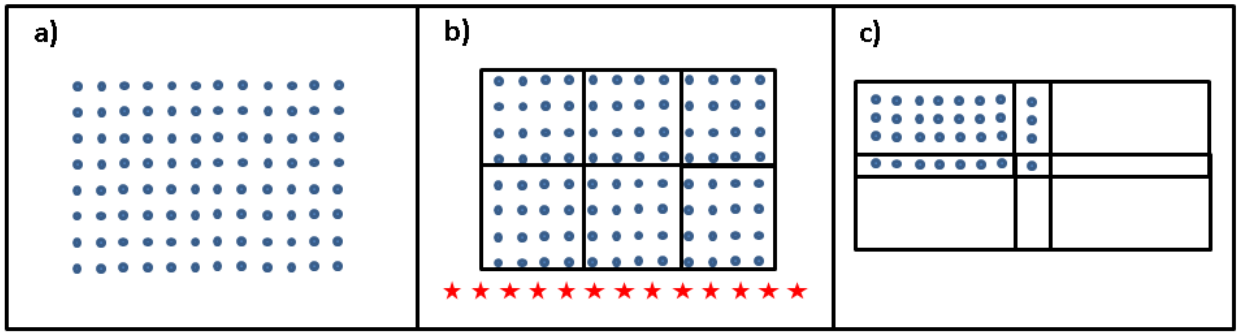

Figure 1: Different methods of creating a plane of complex measurements for use in NAH: a) shows a single plane of measurements taken simultaneously, b) shows scan-based measurements pieced together using stationary reference microphones, and c) shows scan-based measurements stitched together using spatially overlapping measurement positions between adjacent scans.

A novel streamlined method of obtaining a complex pressure field has been developed and is presented in this thesis. This method uses self-referencing between scan-based measurements, removing the costly necessity for stationary reference microphones. Figure 1 part c) shows the overlapping measurement positions between adjacent scans that are used to stitch the phase and amplitude of adjacent scans together. This method relies on a stationary source, and on the local coherence of the pressure between measurement positions, implying a consistent pressure amplitude and relative phase at each location.

This thesis presents the technique by application to a laboratory scale experiment and jet noise data. The method is described in Chapter 2 and requires two steps: unwrapping the phase of individual scans, and stitching together the amplitude and unwrapped phase of adjacent scans using the local coherence between overlapping measurement positions. Chapter 3 explains a laboratory-scale experiment designed to validate the method and presents the resulting stitched complex pressure planes, and supporting results. Chapter 4 illustrates the effectiveness and usefulness of the method when applied to full-scale jet noise, and assesses the potential impact of this technique on future application to NAH.

Chapter 2: Methods

This chapter describes the new method of obtaining a correlated complex pressure field using self-referencing between overlapping regions in scan-based measurements. This method reduces experimental cost and computation time required when using stationary reference microphones. The technique has two major steps: phase unwrapping, and phase and amplitude stitching. The resulting temporally correlated complex pressure array can be used in performing acoustical holography to characterize sources that are difficult to directly measure, such as military jet noise.

2.1 Phase Unwrapping

Complex acoustic pressure measurements contain an amplitude A and phase θ, represented by

$$P = Ae^{-i\theta t}.$$

The phase gives a temporal relationship between measurement positions with values varying over one period, from $-\pi$ to π. This modular representation of phase demonstrates the periodicity of the wave, but fails to capture the phase progression over a long distance. When the aperture is large and many wavelengths fit in the measurement region, it is useful to unwrap the phase to see the relative phase between positions many wavelengths apart. Figure 2 (a) shows the complex pressure phases of a simulated 1-D line array of 250 microphones. Figure 2 (b) shows this same signal with the phases unwrapped, displaying the phase relationship between all microphones in the line array. From the wrapped phase, the spatial periodicity of the wave is clear. From the unwrapped phase, the relationship from the first and last microphone can be calculated to be 30 radians, or about 15 periods. Figure 2 (c) and (d) show this same process applied to a two-dimensional array of data, with analogous results.

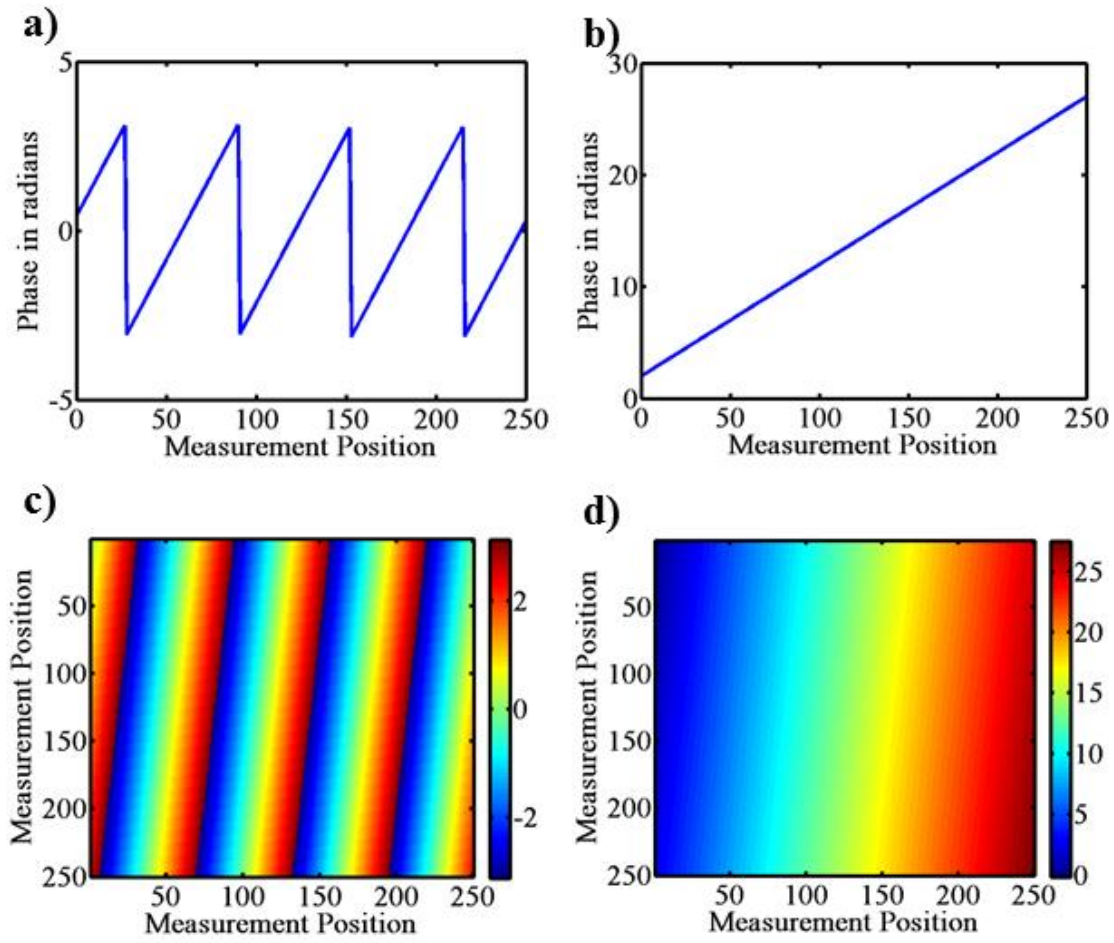

Figure 2: Simulated data representing wrapped vs. unwrapped complex pressure phase. A) Wrapped phase for a 1-D line array of measurement positions. B) Unwrapped phase for the same data, showing continuous phase relationship. C) Wrapped phase for a 2-D array of measurement positions. D) Unwrapped phase for the same 2-D data, showing continuous phase relationship across the array.

2.1.1 The Phase Unwrapping Problem

Basic unwrapping algorithms present a problem for accurate unwrapping. These algorithms isolate and remove "wraps" by first identifying the difference in phase between adjacent measurements. Any difference in phase greater than π is considered to be a wrap, and π is added to the smaller phase. This type of simple algorithm works well for ideal data as shown in Figure 2, but becomes increasingly difficult as the signal-to-noise ratio decreases. Adding noise to the 1-D line array shown in Figure 2 (a) results in the phase data shown in Figure 3 (a). Figure 3 shows that the basic unwrapping algorithm generates errors with applied to the noisy signal.

Methods

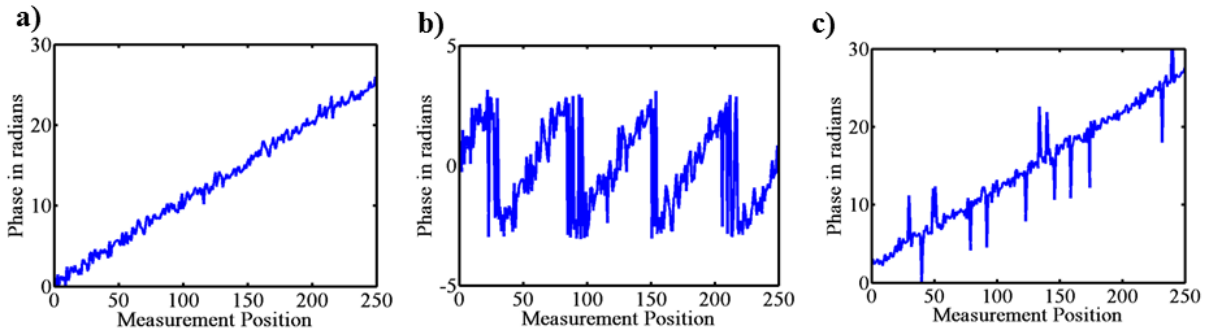

Figure 3: Unwrapping algorithm applied to the phase of a simulated noisy 1-D array. A) Original signal. B) Wrapped signal. C) unwrapping algorithm applied to b) resulting in errors because of the noise.

Expanding the phase unwrapping problem to two-dimensional arrays increases the complexity further[13]. Traditional phase unwrapping follows a continuous path that can lead to large errors when applied to a large, complex two dimensional array. The simple method of two dimensionally unwrapping a phase array is to first sequentially unwrap each column as a one dimensional array and then unwrap each row (or vice-versa). This straightforward method works well for datasets that are free from any noise or errors; however, any errors contained in the signal are propagated throughout the scan amplifying the problem and resulting in gross inaccuracies. Figure 4 shows the propagation of errors that results from the row-then-column method applied to a noisy signal.

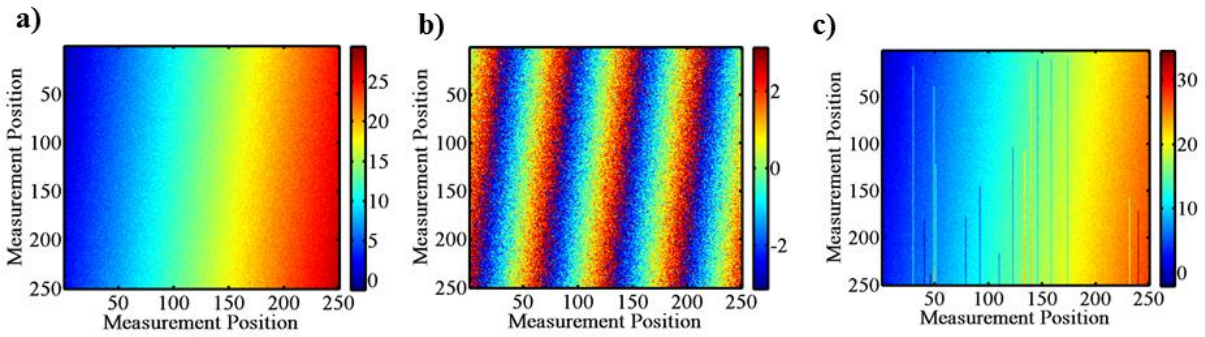

Figure 4: Unwrapping algorithm applied to the phase of a simulated noisy 2-D array. A) Original signal. B) Wrapped signal. C) Unwrapping algorithm applied to b) resulting in errors because of the noise.

Signal errors that can lead to propagated discontinuities are signal noise, under sampling (spatially or temporally), and abrupt phase changes inherent in the sound field.[14] All of these challenges are present in jet noise data. Signal noise is an inherent feature of jet noise as it is a partially correlated turbulent source. The spatial sampling of jet noise is 6 inches, making the spatial Nyquist frequency about 1,000 Hz . Lastly, abrupt phase changes in the sound field are present due to ground reflections. These cannot be unwrapped accurately using simple algorithms.

2.1.2 Solution to the Two-Dimensional Phase Unwrapping Problem

The two dimensional unwrapping problem can be solved using an algorithm developed by the General Engineering Research Institute at Liverpool John Moores University.[15] Their "fast, two-dimensional phase-unwrapping algorithm, based on sorting by reliability, following a non-continuous path" or 2D-SRNCP unwrapper was developed for unwrapping optical images. The algorithm has been applied to

Synthetic Aperture Radar and Magnetic Resonance Imaging, and now to scan-based acoustic measurements. The 2D-SRNCP uses computationally efficient methods to successfully unwrap the phase of two-dimensional signal arrays that contain noise, phase discontinuities, and under sampling.

The 2D-SRNCP algorithm uses a non-continuous path to avoid propagating discontinuities over the length of a measurement plane. Phase differences between adjacent measurement positions are calculated. First the measurement positions requiring no unwrapping are fixed relative to one another. Then the differences between adjacent positions that are near π will be unwrapped. Large, isolated, or unclear jumps are unwrapped last. This dis-continuous unwrapping path is quality-guided and prevents errors or discontinuities from being propagated throughout the scan as they are with a row-then-column approach (see Figure 4 for a reminder of what error propagation looks like).

This algorithm has been successfully applied to scan-based acoustic pressure measurements made in a laboratory as well as in the field. An example of the successful unwrapping of a noisy acoustic signal is shown in Figure 5. The data used to generate Figure 5 was a plane of complex pressure phase at a single frequency shown in the top plot which contains 2π jumps. Applying the 2D-SRNCP algorithm to the data creates the bottom plot – a smoothly unwrapped scan of continuous phase.

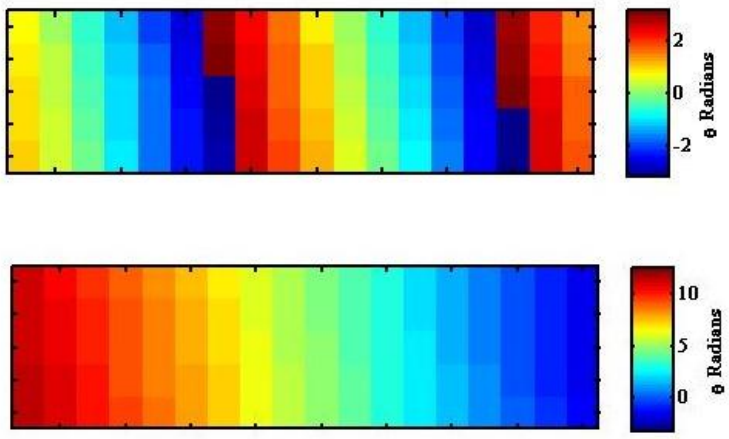

Figure 5: Illustration of successful two dimensional phase unwrapping. The top figure shows the phase of a single frequency, single block complex pressure varying between $-\pi$ and π. The bottom figure is the same signal unwrapped using the 2D-SRNCP unwrapper described in reference15.

A scan with continuously unwrapped phase is ready to be used in NAH, or to be stitched together with other scans if a larger aperture is necessary. An example of several adjacent scans in a scan-by-scan measurement array with phases unwrapped is shown in Figure 6. This is what the phase of overlapping scans such as those shown in Figure 1 (c) would look like. The black lines indicate the regions where the microphone positions overlap between adjacent scans. This figure shows that although the phase across each scan is continuously unwrapped, the phase relationship between the overlapping measurement positions is not consistent. This illustrates the need for phase stitching between adjacent overlapping scans to create a large coherent complex pressure plane.

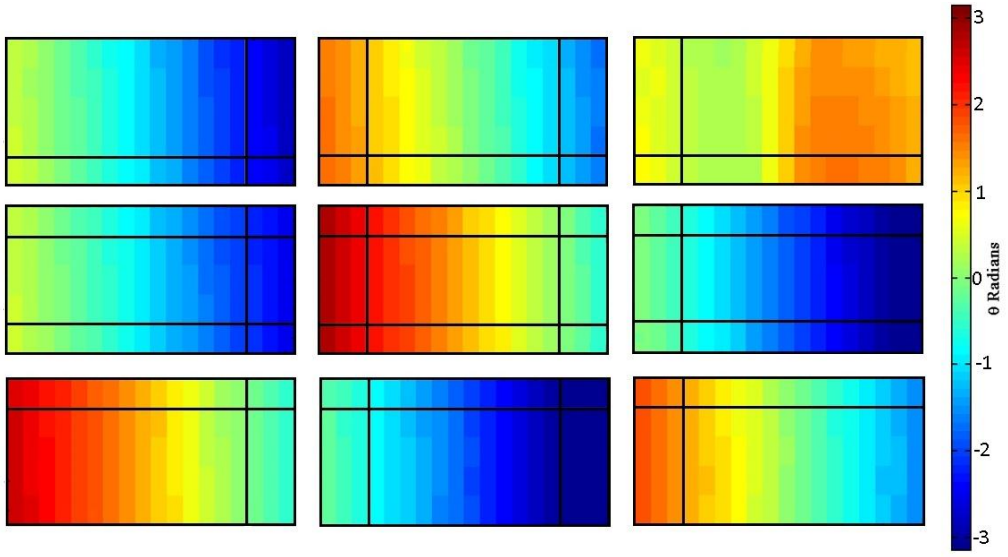

Figure 6: Illustration of adjacent scans of single frequency, single block complex pressures with phases unwrapped. The black lines indicate regions of spatial overlap between scans. This shows the necessity of phase stitching between scans to create one phase-aligned array of measurements.

2.2 Phase and Amplitude Stitching

2.2.1 The Stitching Problem

The objective of "stitching" is to combine small scan based measurement arrays into one large coherent array. When stitching between measurement scans, it is imperative that the intra-scan phase relationships be maintained while the total phases are shifted to match the edges. This is done by calculating a single scalar phase and magnitude shift to apply to each scan, preserving the phase across each scan while allowing the overlapping regions to align. Calculating a single scalar shift becomes difficult for a 2-D grid of scans such as Figure 6. For the center scan in that array there are 8 overlapping regions: 4 sides, and 4 corners of the scan that overlap with the 4 adjacent scans and 4 cornerwise scans. Aligning all of these overlapping regions to make a continuous scan is extremely difficult.

Additionally, the total energy across the aperture of measurements must remain unchanged by the data processing. As amplitudes are stitched together across scans and averaged over blocks, the total energy cannot be erroneously altered. Both of these issues have been solved by the stitching algorithm presented here. The method will be explained thoroughly in this section, and will be applied tutorial-style to laboratory acoustic data in section 3.4.1.1.

2.2.2 Solution to the Stitching Problem

The solution to the stitching problem is presented in this section. The solution begins with the Fourier computation of complex pressures. Complex pressures are computed using the time varying wave form for individual time blocks and frequency bins. The complex pressure at each microphone position is represented by the equation $P = Ae^{-i\theta}$, with an amplitude and phase for each bin and block. Full scans of unwrapped complex pressure phases still represent just one frequency and one time block. These phases are stitched together and then ensemble averaged across all blocks after they have been stitched. Amplitudes are stitched together after ensemble averaging all time blocks. Resulting complex pressure planes represent one frequency bin.

To stitch together the complex pressure amplitude to create a single plane, first the magnitude of each microphone is averaged over all blocks. These ensemble-averaged amplitudes are then stitched by replacing the overlapping positions' amplitudes with the average between the measurements taken at each position. Inner scan positions are unaltered. The result is a large array of complex pressure amplitudes that will be combined with the stitched complex pressure phases to create a continuous, coherent array of complex pressures. Stitching the amplitude is far simpler than stitching the phase.

The schematics in Figure 7 and Figure 8 illustrate the phase stitching process. A reference scan, in this example the center right, is chosen near the most correlated source region and the phases in all other scans are shifted by scalars relative to the reference scan. The phase difference between the reference scan and its adjacent scans is calculated using the overlapping microphone regions. In Figure 7, the scans above, below, and to the right of the reference scan are shifted first. The phase difference $\delta\theta$ between each pair of microphones in an overlapping position is calculated, and the median difference for an overlapping region is calculated. This median phase difference is then subtracted from the adjacent scan. In Figure 7, for example, the median of all the $\delta\theta$ in the upward direction is $\delta\varphi_{t1}$. This is the scalar shift subtracted from the top right scan. The same process is applied the other scans adjacent to the reference scan.

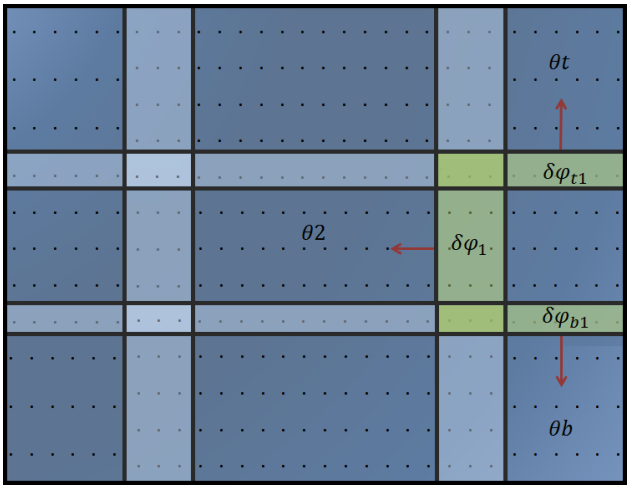

Figure 7: Diagram showing the first step of the self-referencing phase stitching process. A reference scan (in this case the center right) is chosen in a region of relatively high source correlation. The difference between microphones at each measurement position is calculated then the median difference is found for each overlapping region (top, bottom, and leftward). Each phase difference is subtracted from the subsequent scan.

To shift a single scan in the middle of a two-dimensional array of scans, the information from all preceding scans must be used. This is done by considering all overlapping regions from the preceding scans that have already been stitched to the reference scan. Consider the top center scan in Figure 8. The preceding scans that have been stitched are the center right, top right, and center scans. The median phase difference for each overlapping region is calculated in the same method described above, and then the median of those shifts is subtracted from the center top scan. The center top scan is now continuous with all three scans preceding it. This method is far more effective than stitching in only one dimension because, similarly to the unwrapping problem, small errors can be amplified and propagated when many scans are stitched in a row. This method is continued until the phase of the entire array of scans is stitched relative to a single reference scan.

Methods

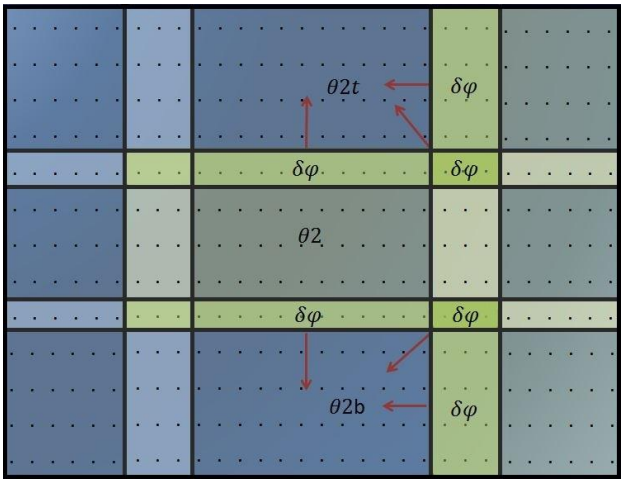

Figure 8: Diagram showing the second step of the self-referencing phase stitching process. Each scan moving left has three scans that have been shifted before it: a vertical, horizontal, and diagonal one. A shift is calculated using the median phase difference in each direction.

After the complex pressure phases of all scans are stitched together to create the full in-phase array for individual blocks, the array needs to be ensemble averaged over the time blocks. The fully stitched phase arrays for every time block need to be zeroed out at the same position. It does not matter which position is set to zero, because the relative phase will be preserved. With all blocks set to the same relative reference, the average across blocks is taken. This process creates a complex pressure phase that represents the entire signal. The averaging process removes any small phase discontinuities that remain after the unwrapping and stitching processes.

The phase correlated plane has been created out of scan-by-scan measurements without the use of stationary reference microphones. The final complex pressures are generated by combining the stitched and averaged amplitude A and phase θ at each position by $= Ae^{-i\theta}$. Stitching a plane of scan based measurements using this self-referencing algorithm provides a large two-dimensional plane of spatially correlated complex pressures that can be used for phase dependent analysis. For an example of how this unwrapping and stitching method is applied to laboratory data, see Appendix 1.

Chapter 3: Laboratory Experiment

This experiment was designed with the end goal of simulating performing NAH on full-scale military jet noise using a coherent measurement plane stitched together using self-referencing between overlapping scan based measurements. The efficacy of this experiment leads to promising prospects of reducing time and expense in more costly full-scale military jet noise tests in the future. These tests will lead to insight into the characteristics of the jet noise source and ultimately lead researchers to reduce hearing loss among military personnel.

3.1 Measurements

In January 2014, acoustic pressure measurements of a line source with varying correlation were made in a fully anechoic chamber at Brigham Young University. The anechoic chamber facility has working dimensions of 8.71 x 5.66 x 5.74 m, and an anechoic frequency range of 80 Hz to 20 kHz. Performing a controlled test in an anechoic chamber eliminates ground reflection interference that leads to phase discontinuities. A phase discontinuity inherent in the data is nigh impossible to unwrap correctly with the methods used here, so for developmental purposes the ground reflection was undesirable.

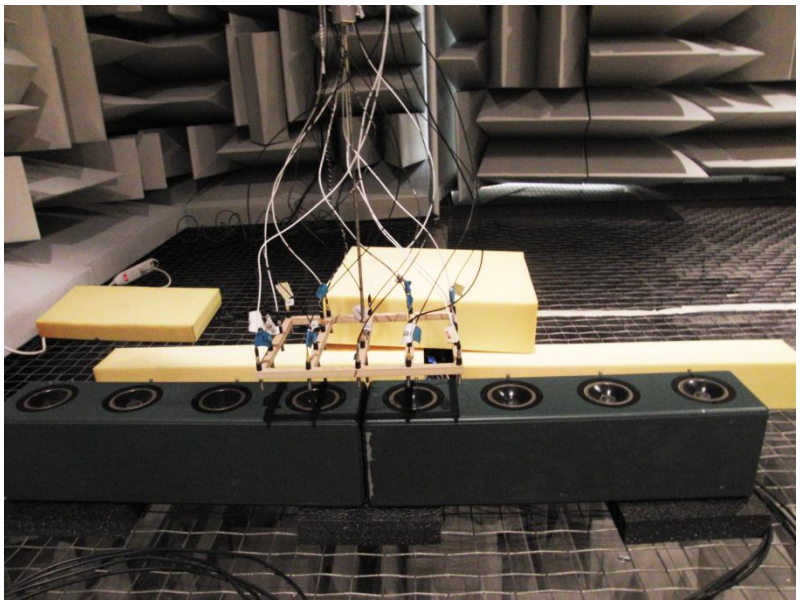

Figure 9: Picture of the line array of 8 loudspeakers driven by 4 dual output amplifiers. Also pictured is the 20- microphone array used to take scan-based measurements.

Data acquired in this experiment were taken on a small rectangular array of 20 GRAS 40 BE ¼" free-field microphones. Microphones were placed in a 5 X 4 CNC-milled wooden grid with 3" microphone spacing in each direction seen in Figure 10, creating a 12 X 9" array. The array was placed with the longer dimension (15") running parallel to the line source to minimize the number of scans needed to adequately cover the source aperture. Additional ¼" pressure microphones were placed near each loudspeaker as stationary reference microphones for use in future comparison in performing NAH using complex pressure planes computed using both the self-referencing and reference microphone methods.

Laboratory Experiment

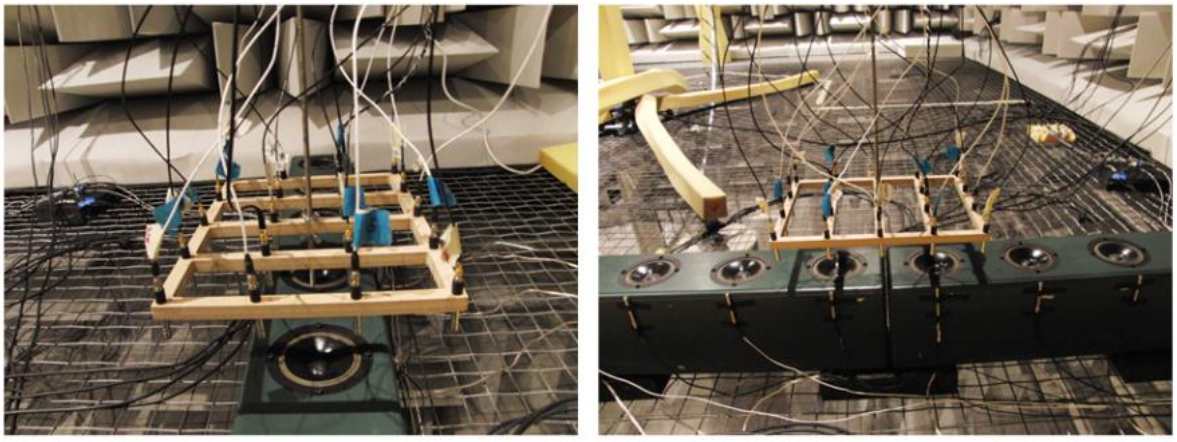

Figure 10: Picture of the measurement rig holding 20 free field microphones in a plane parallel to the line- array. The rig is attached at the center to an automatic positioning system in the anechoic chamber allowing for accurate movement between scans. Reference microphones attached to the line source are seen in the right picture.

To acquire data, an automated positioning system (APS) was used to move the measurement array to 21scan positions in a 3 X 7 pattern. These positions included overlapping microphone positions between adjacent scans. These scans of 20 microphones with the overlapping regions result in 230 unique measurement positions arranged in a 23 X 10 microphone array spanning a 69 X 30" region. Figure 11 shows a schematic of the complete measurement array, with overlapping regions indicated by the grey stripes.

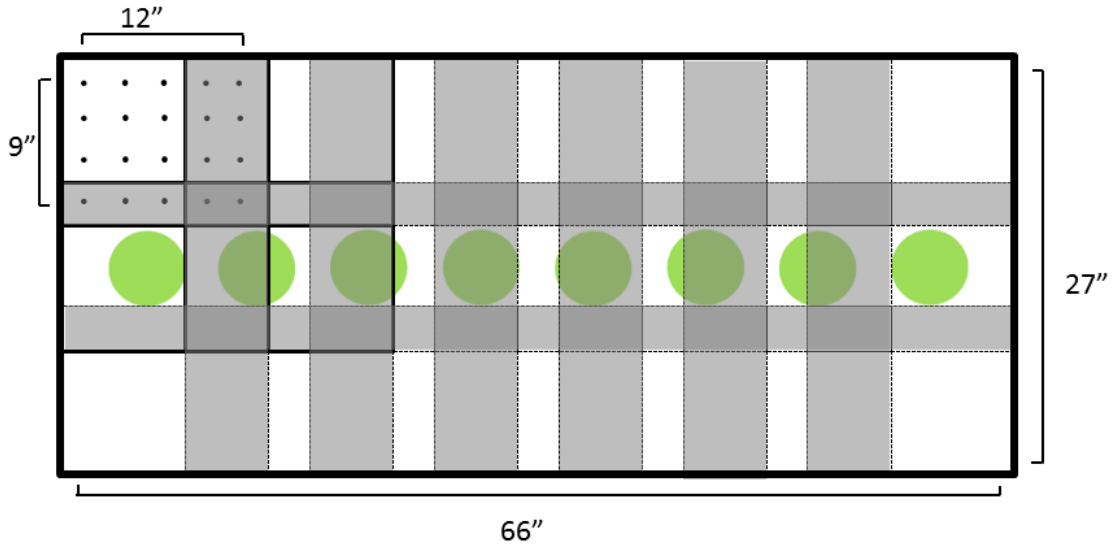

Figure 11: Diagram representing measurements of a line array taken in an anechoic chamber at Brigham Young University. Each small dot represents one microphone in a scanning 5 X 4 the measurement rig containing 20 free-field microphones with 3" spacing. The measurement rig was moved to 21 scan positions, creating 230 unique microphone positions. Grey regions represent areas of spatial overlap between scan positions. Two microphones were overlapped in the horizontal direction, and one in the vertical direction. The large green dots represent the 8 loudspeakers comprising the line array used to generate various source conditions.

These overlapping regions will be used to self-reference between measurement scans because of the local coherence of the noise between measurement positions. If the coherence is sufficiently high, we can assume that the complex pressure amplitude and relative phase of data recorded at different times in the

same position will be the same. The high local coherence is demonstrated for this experiment below in Section 3.3.

The microphone array was positioned at two heights, 1" and 6", from the source. The data at 1" will be useful as a benchmark to test the effectiveness of a near-field acoustical holography application. Using the 6" data, acoustical holography will generate the sound field at 1" from the source using inverse methods. Comparing this hologram to the actual 1" data will be another way to validate the method. This will possibly be used in future work for rigorous validation of the stitching algorithm.

3.2 Source Conditions

The acoustic source used in this laboratory experiment was a line array of eight 3-1/2", 290-210Watt loudspeakers driven with signals of varying correlation. The line array is pictured in Figure 9. The source conditions were 1) a 100 Hz sawtooth, 2) correlated 100-1000 Hz white noise, 3) partially correlated 100-1000 Hz white noise, and 4) uncorrelated 100-1000 Hz white noise.

Correlated white noise and a sawtooth signal provide similar acoustic conditions, except for the frequency content, which is broadband for the white noise but contains only harmonics of the 100 Hz fundamental for the sawtooth. Figure 12 gives a representation of the perfect source coherence. Measurements made at any position above the line source are equally coherent to all source reference microphones.

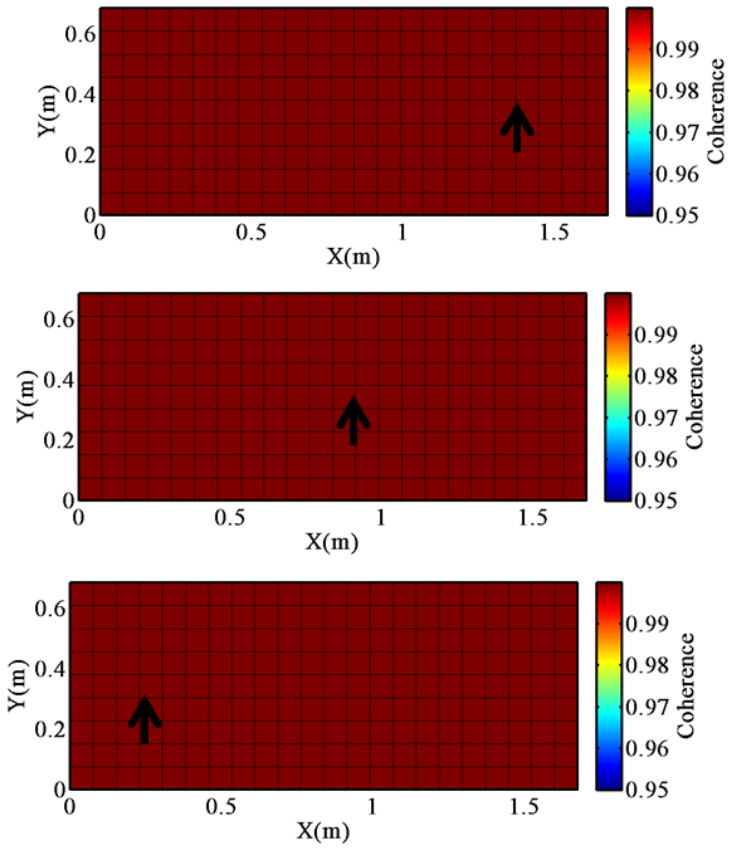

Figure 12: Coherence between every microphone position in the scan-based array and the reference microphone near the source indicated by the arrow for the sawtooth source condition. The source condition here is a sawtooth signal. Reference microphones are pictured in Figure 9. The coherent white noise signal produces the same level of perfect coherence across the entire scan.

Laboratory Experiment

Partial correlation was achieved by selecting one random white noise signal to be the reference. Reference, "signal 1" was sent to source 1. The second source contained 50% of the first signal, mixed with 50% random uncorrelated white noise. The third source contained 25% of the first signal mixed with 24% of the second signal, and 50% random uncorrelated white noise, and so on. This partially correlated condition resembles jet noise with uncorrelated and correlated components of the signal all along the source, but predominantly uncorrelated noise near the jet exhaust and predominantly correlated noise farther downstream. The partially coherent source model was developed by A.T. Wall in Reference 9.

Table 1: Table showing unique signal components contributing to each source in a partially correlated line source model.

	Source 1	**Source 2**	**Source 3**	**Source 4**	**Source 5**	**Source 6**	**Source 7**	**Source 8**
Signal 1	1	1/2	1/4	1/8	1/16	1/32	1/64	1/128
Signal 2	0	1/2	1/4	1/8	1/16	1/32	1/64	1/128
Signal 3	0	0	1/2	¼	1/8	1/16	1/32	1/64
Signal 4	0	0	0	½	1/4	1/8	1/16	1/32
Signal 5	0	0	0	0	1/2	1/4	1/8	1/16
Signal 6	0	0	0	0	0	1/2	1/4	1/8
Signal 7	0	0	0	0	0	0	1/2	1/4
Signal 8	0	0	0	0	0	0	0	1/2

The resulting partial correlation is seen in Figure 13. "Source 1" was positioned on the right side of the scan, and has a wider region of high coherence. "Source 8" was positioned on the left side of the array, and has a much narrower region of high coherence.

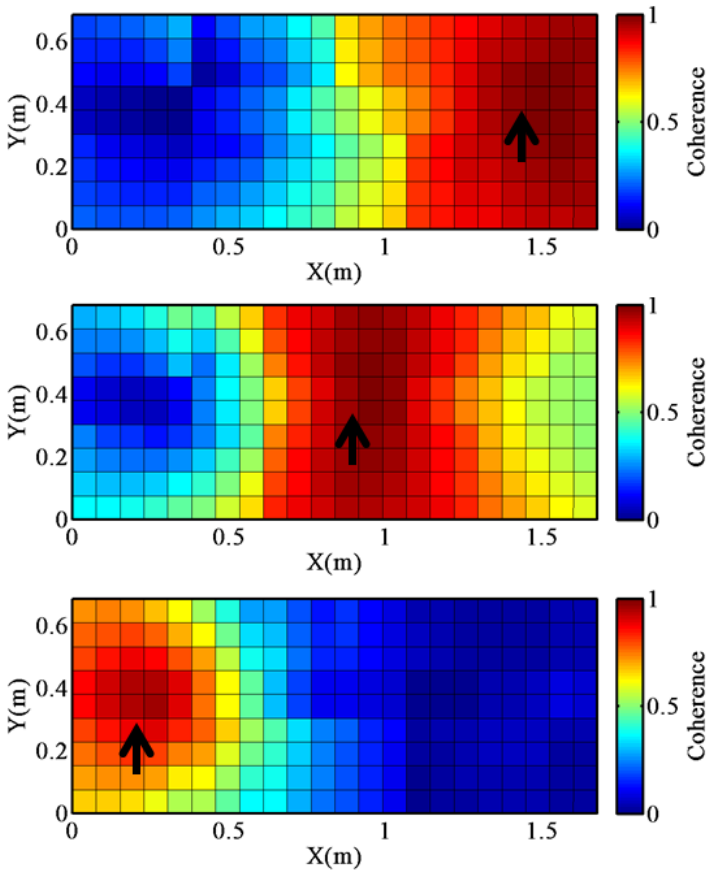

Figure 13: Same as Figure 12, but for the partially coherent white noise source condition. The coherence in the top plot was calculated with reference to the region of highest source coherence, and there is a wider region of high coherence on the measurement array than the bottom plot whose reference was in the region of lowest source coherence.

The incoherent white noise source condition was generated by driving each loudspeaker with a statistically unique white noise signal. Although the sources comprising the line array are completely incoherent from one another, the measurement array's geometry is such that there is still local coherence between measurement positions (Figure 14). In other words, several adjacent microphones receive enough of the signal from the same loudspeaker that their relative coherence is high. This will positively impact the effectiveness of stitching incoherent noise in this experiment as seen in section 3.4.

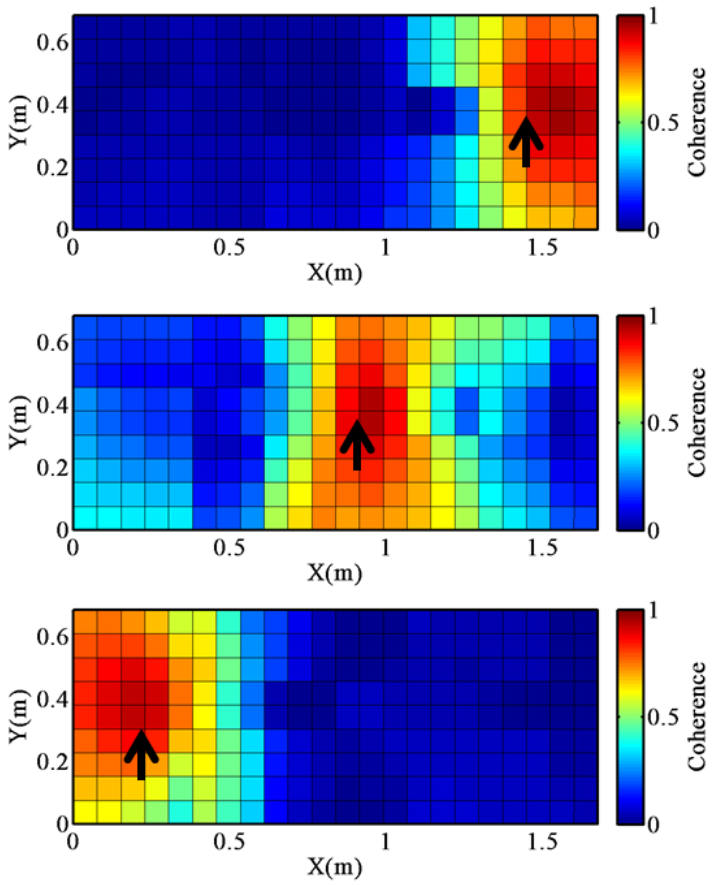

Figure 14: Same as Figure 12, but for the incoherent white noise source condition. The regions of high coherence corresponding to regions where adjacent microphones are receiving predominantly one source's signal are much smaller than those in the partially coherent source condition shown in Figure 13. There is still sufficiently high local coherence for stitching.

3.3 Meeting Source Requirements

As described in section 2.2, assumptions about the source were made in order for the stitching technique to be applied. The source must be stationary enough (producing a consistent sound field over time) that the relative phase and amplitude between microphones in the overlapping region is the same from scan-to scan. For example if measurements with two microphones are made at two different times, they must have the same phase and amplitude relationship. In order to validate these source assumptions, coherence analysis is used. If local coherence between microphone positions is high, then the source has sufficient stationarity, and scan-by-scan measurements can be stitched using self-referencing.

Coherence γ^2 is calculated using the equation

$$\gamma^2 = \frac{|Gxy|^2}{G_{xx} * G_{yy}}.$$

Where $G_{xx} = \langle CP^* * CP \rangle$, $G_{yy} = \langle {CP_{ref}}^* * CP_{ref} \rangle$, and $G_{xy} = \langle CP^* * CP_{ref} \rangle$.

The variable CP is the complex pressure at one microphone, and CP_{ref} is the complex pressure at the reference microphone. The averages are taken over all blocks.

One way to assess local coherence is to look at the coherence between the source and the measurement array using reference microphones. This analysis is presented in section 3.1 in Figure 11 through Figure 14. These plots show that adjacent microphones receive acoustic signals that are composed of predominantly a single source in the line array. While this gives an indication that local coherence is high, it doesn't actually show the signal relationship between adjacent microphone positions, or that the signal relationship between adjacent microphones is consistent from scan to scan.

A more rigorous technique for validating the assumption of local coherence is to calculate the coherence between adjacent microphone positions present in multiple scans. Figure 15 illustrates how two microphone positions (stars) are present in four overlapping scans (A1-A4). The coherence between the microphones was calculated for each of the four scan positions. The result is four coherence values which, if consistent, indicate both high local coherence and source stationary. This same analysis was performed for region B indicated in the plot. Regions A and B are temporally unrelated. If they have similar and high local coherence, this will indicate that there is enough local coherence throughout the measurement array to stitch the entire array together.

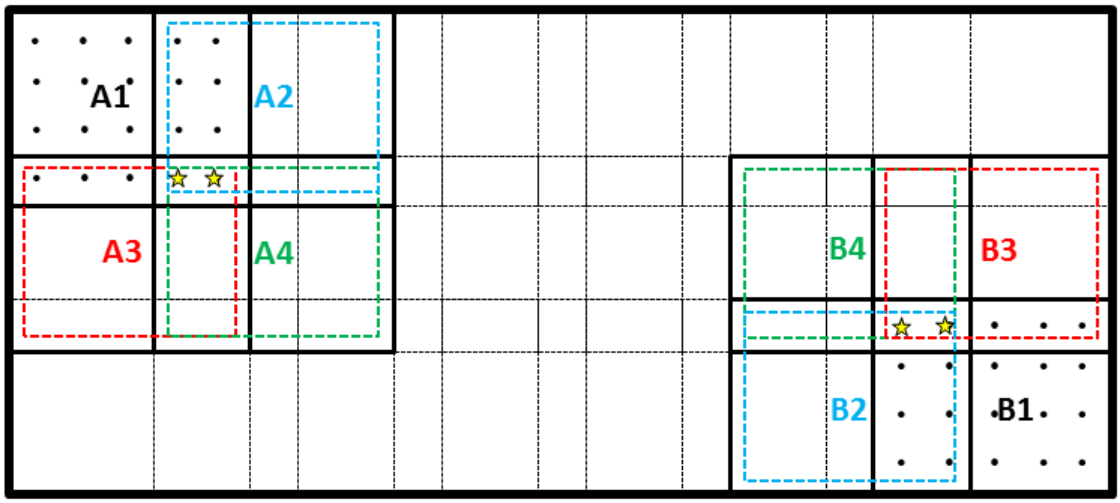

Figure 15: Schematic illustrating microphone positions used to calculate local coherence between adjacent microphone positions. The stars indicate adjacent microphone positions at spatial locations present in 4 adjacent scanning array positions. Signal coherence was calculated between the starred microphones for each of the 4 scans that overlap in that region. A consistently high coherence value indicates strong local coherence and source stationarity. Results from this analysis are presented in Table 2.

The results from this analysis are shown in Table 2. The correlated white noise and sawtooth source conditions present similarly high local coherence between adjacent microphone positions for all scans. Partially correlated and uncorrelated noise source conditions have a slightly lower local coherence. Despite the lower local coherence, the consistency from scan to scan is high, and all coherence values are above 0.9, meaning that they are high enough to assume a consistent phase and amplitude relationship within the overlapping regions between scans. These values show that the local coherence is high enough to meet the source assumptions required to perform the unwrapping and stitching techniques presented in Chapter 2.

Table 2: Local coherence between two starred microphone positions contained in 4 overlapping scanning array positions. Two array positions are recorded, A and B (shown in Figure 15). Results are presented by source condition.

Coherence	Correlated Noise	Partially Correlated	Uncorrelated	Sawtooth
A1	.9999	.9791	.9525	1
A2	.9993	.9809	.9715	.9999
A3	.9999	.9805	.9600	1
A4	.9999	.9801	.9688	1
B1	1	.9961	.9576	1
B2	1	.9954	.9723	1
B3	.9991	.9919	.9485	.9998
B4	1	.9942	.9600	1

3.4 Results

Results from the laboratory experiment demonstrating the creation of coherent complex pressure planes are presented in this section. A full description of the stitching methods is given in section 2.2; but for the first test condition, results are given as a step-by-step tutorial to demonstrate how the method is implemented. The subsequent results are presented with only the final product and any steps that are of particular interest. Results are presented first by source condition, then by frequency, and lastly by measurement plane height. Finally, the results are validated using coherence analysis.

3.4.1 Source Comparison

3.4.1.1 Partially Correlated White Noise

While other source conditions give insight into the method's validity, the partially correlated condition is of most interest because partially correlated white noise is most closely representative of jet noise. To simulate jet noise, this signal had varying correlation between each speaker. The speakers moving "upstream" had an increasingly small percentage of the first speaker's signal. This reflects jet noise which has regions of higher correlation farther downstream from the jet exhaust.

The complex pressure amplitudes of the line source driven by a partially uncorrelated signal wave as measured on a scan-by-scan basis at 6" from the source are shown in Figure 16. Each pixel represents one microphone position within the array. One row and two columns overlapped position, and accordingly have similar amplitudes, between scans. This overlap can clearly be seen Figure 16.

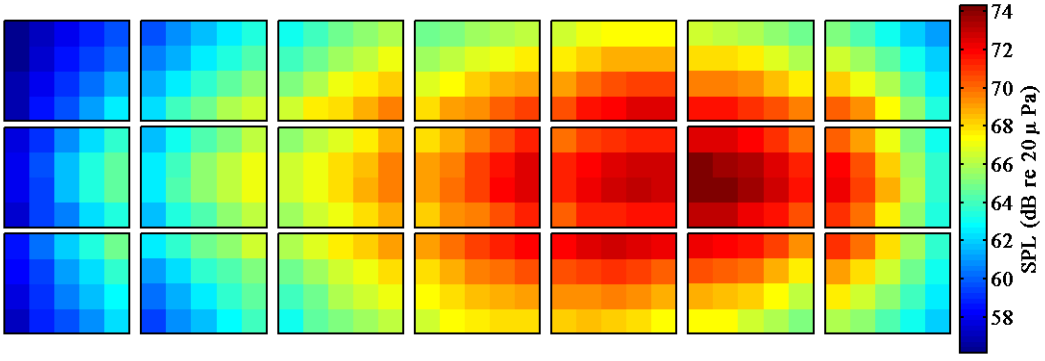

Figure 16: Amplitude of 200 Hz data from measurement scans of the 8 microphone line-array driven with a 100-1000 Hz partially uncorrelated signal. Each square of data represents one scan position and each pixel represents one microphone position. One row and two columns overlap position between adjacent scans.

To stitch together the complex pressure amplitudes, first the mean-squared complex pressure amplitude measured at each microphone position is averaged over all blocks. Stitching the amplitudes is accomplished by creating an array with the unique measurement positions unaltered, and each overlapping measurement position being represented by the average of the two complex pressure amplitudes recorded in that position. If $A1$ and $A2$ are the amplitudes of the complex pressures recorded at the same measurement position in scan 1 and scan 2, then the amplitude used to represent that measurement position is $A = (mean(A1, blocks) + mean(A2, blocks))/2$. The stitched, averaged amplitude for this condition is shown in Figure 17.

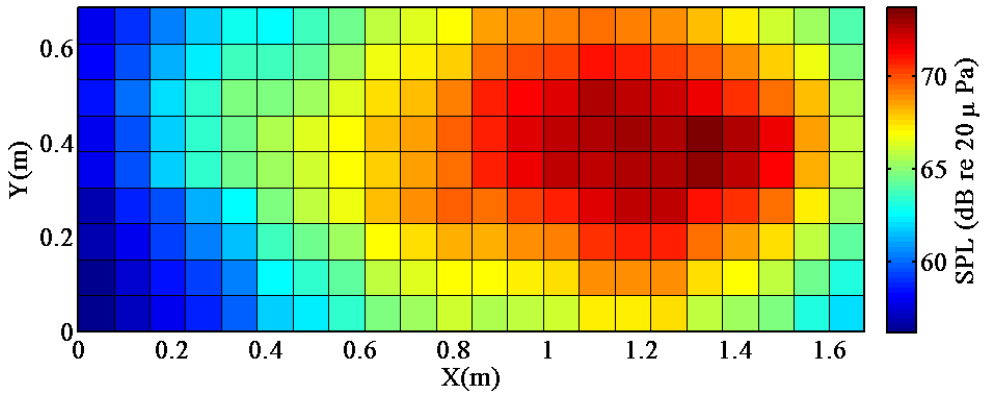

Figure 17: Amplitude of 200 Hz data from measurement scans of line-source driven with a 100-1000 Hz partially uncorrelated signal. Amplitude has been averaged over all blocks and stitched together maintaining the same overall energy. This represents the complex pressure magnitude for a 21-scan plane of data.

With the amplitude successfully stitched, the more complicated process of unwrapping and stitching the phase can be addressed. The phase is unwrapped and stitched one frequency and one block at a time, before being ensemble averaged by blocks for each frequency. Every scan will have a phase independent of the other scans due to the temporal separation of the measurements. When complex pressures are calculated using Fourier methods, the result is a unique phase varying from $-\pi$ to π for each measurement position.

Figure 18 shows these complex pressure phases for 200 Hz data, for a single random time block. Each rectangle of data is one array position, and each pixel is the phase of the complex pressure recorded at a single microphone. The two important features of this plot are 1) the phases of adjacent scans have no relationship to one another because they were taken at different times, and 2) There are discontinuities where the phase jumps from $-\pi$ to π modularly. To find the total phase relationship between every microphone position, the phase for each scan must be unwrapped, then the intra-scan phases can be stitched together using the spatial coherence found in section 3.3 between overlapping microphone positions.

Laboratory Experiment

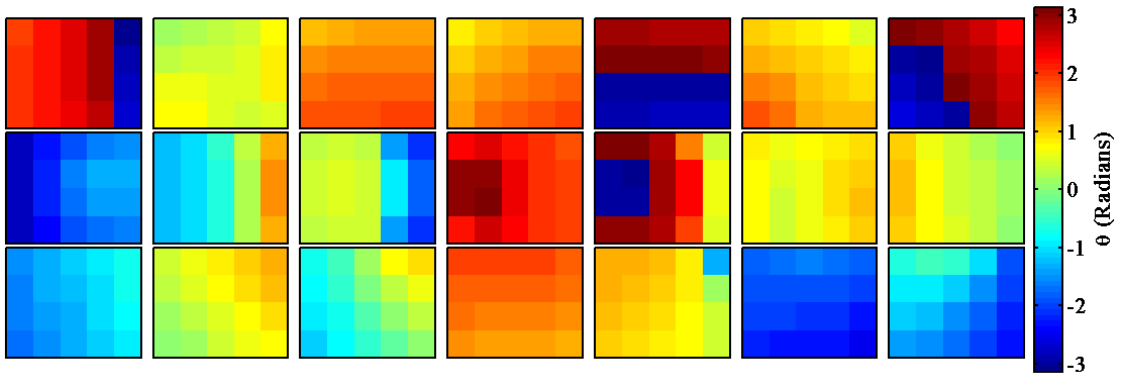

Figure 18: Complex pressure phase of 200 Hz data for a single block. Measurement scans were taken of the 8 microphone line-array driven with a 100-1000 Hz partially uncorrelated signal. Each square of data represents one scan position and each pixel represents one microphone position. One row and two columns overlap position between adjacent scans. Phase is extracted from the complex pressure and us not yet unwrapped or stitched together.

With the unwrapping and stitching method completed on the complex pressure phases for each block, the resulting phase arrays are not perfectly smooth. This is due to the small block size, and noise in the signal. These discontinuities will be removed during the ensemble averaging process. First each block's phase array is zeroed out in the same position. This removes the arbitrary starting phase. Then the array is averaged over all blocks. Figure 19 shows four representative blocks with complex pressure phases stitched together for the 200 Hz partially correlated source condition, before they are zeroed and ensemble averaged.

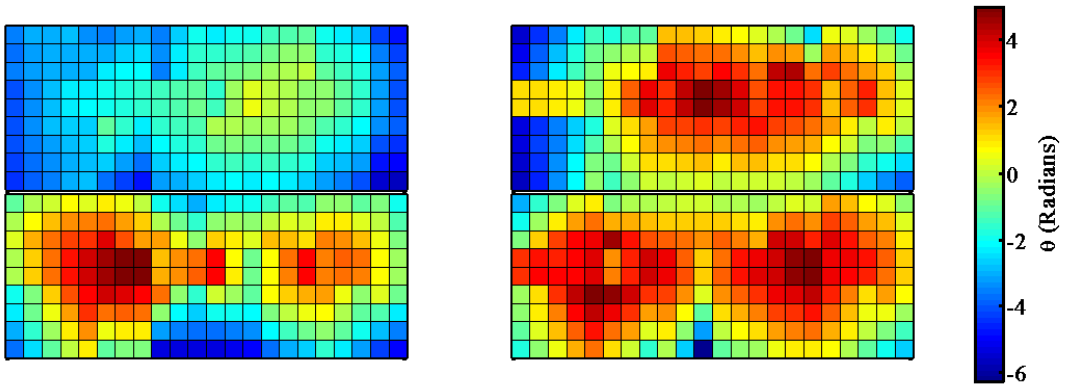

Figure 19: Unwrapped and Stitched complex pressure phases for a plane of data measuring a partially correlated source at 200 Hz. Measurements were taken 6" away from the source. Shown here are the phases of 4 representative blocks. There are still discontinuities in phase that will be averaged out when the blocks are ensemble averaged together prior to use in NAH.

The resulting ensemble averaged complex pressure phase is shown in Figure 20. This array of phase, θ, will be combined with the amplitude A, shown in Figure 17 using $CP = Ae^{-i\theta}$ to generate the correlated stitched complex pressures to be used in NAH. Recall that both the phase and amplitude stitching has been completed without using costly additional reference channels.

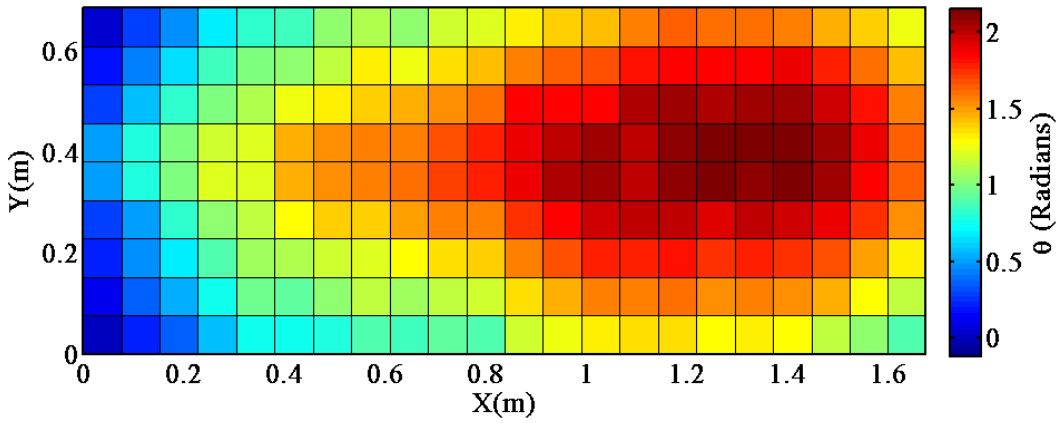

Figure 20: Unwrapped and stitched complex pressure phase for 200 Hz data from the partially corraelated source condition. Measurement plane is positioned 6" from the source.

3.4.1.2 Sawtooth

The sawtooth source presents an esoteric but non-physical demonstration of the stitching algorithm's effectiveness. To more accurately describe jet noise; more complicated broadband sources are used, such as the partially coherent source described above. The sawtooth source exhibits a horizontally uniform acoustic field than the partially incoherent source (see Figure 12 in section 3.2). An additional feature of the sawtooth source is that each time block is nearly identical, see Figure 21 (a). This is because the same periodic signal is sent to each source.

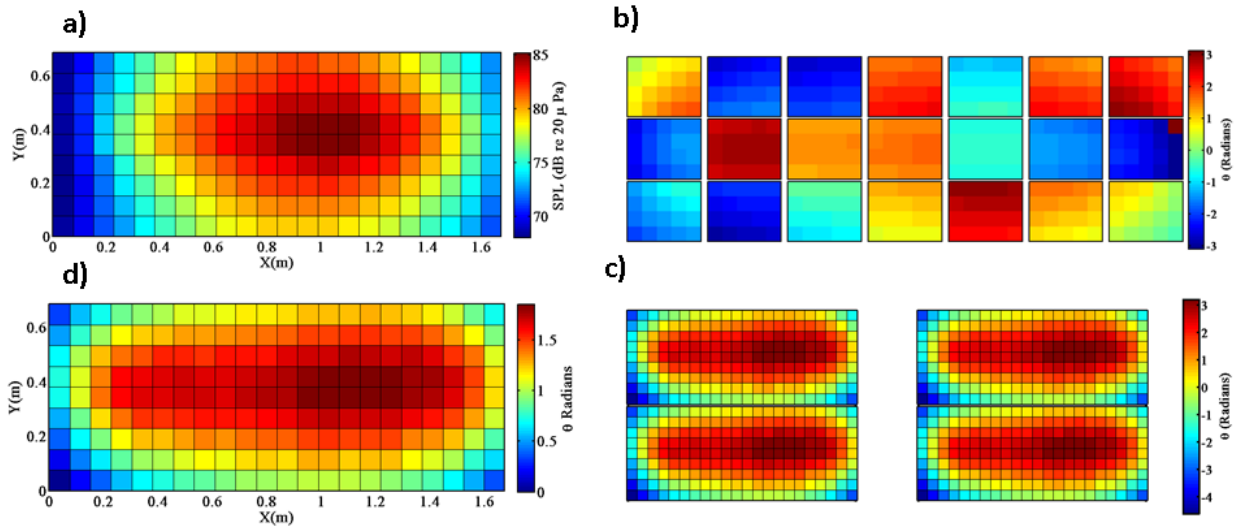

Figure 21: Stitching method and results for sawtooth source measured at 6" at 200 Hz: a) averaged and stitched complex pressure amplitude; b) complex pressure phases of each measurement scan; c) unwrapped and stitched complex pressure phase for the entire plane of data for four representative blocks; d) unwrapped, stitched, and ensemble averaged complex pressure phase for entire data plane. Figure 16 through Figure 20 and the corresponding explanations are the corollaries to each of these plots.

3.4.1.3 Correlated white noise

The correlated white noise source is comprised of a broadband white noise signal from 100 to 1000 Hz, sent to all 8 source loudspeakers. This source creates essentially the same conditions as the sawtooth

(correlated), but it is broad band and non-periodic, instead of harmonic and periodic. Each time block is still remarkably similar.

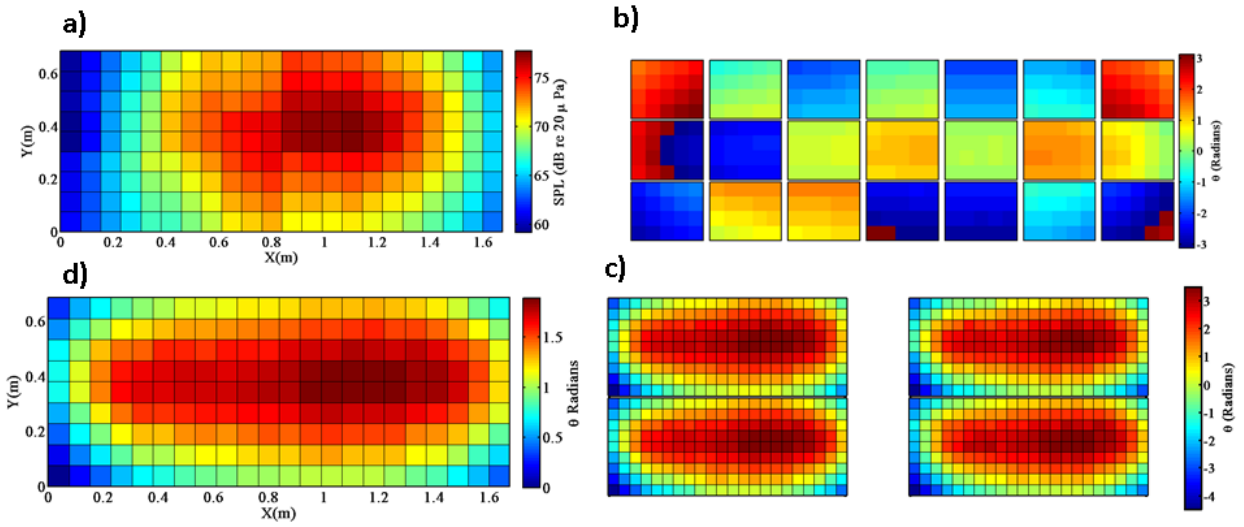

Figure 22: Same as Figure 21 but at the correlated white noise source condition.

3.4.1.4 Uncorrelated white noise

To explore the need for partial source correlateion, uncorrelated white noise was used. Each loudspeaker is driven with a different broadband white noise signal from 100 Hz to 1000 Hz. Individual blocks contain many discontinuities, but the overall stitching still works well. This is likely due to the array being near enough to the source that there is local correlation between the microphones from the same loudspeaker signal that outweighs the uncorrelated components from adjacent speakers.

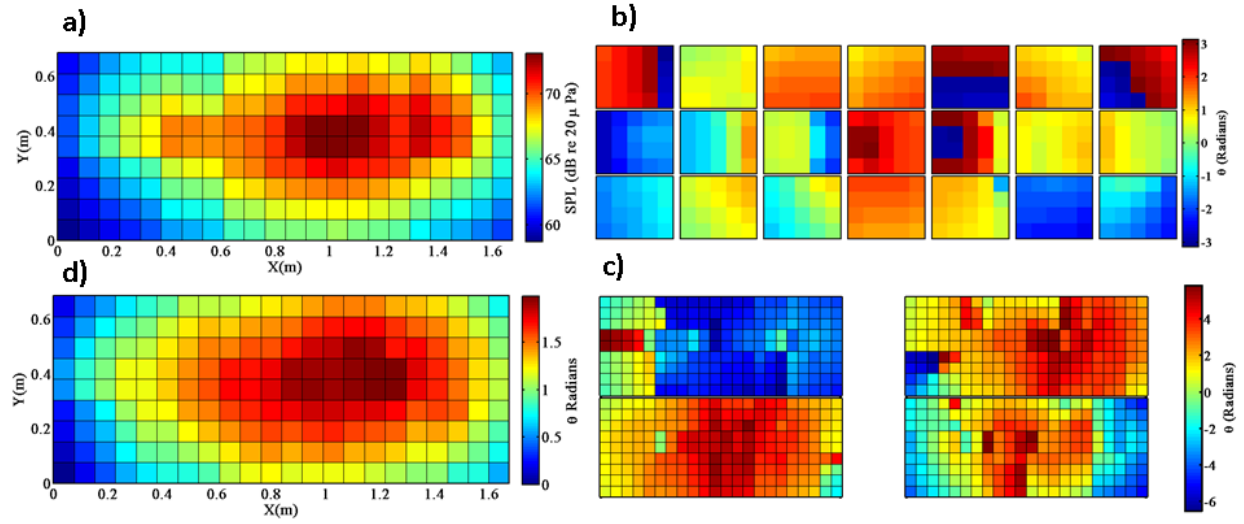

Figure 23: Same as Figure 21 but at the uncorrelated white noise source condition.

3.4.2 Frequency Comparison

As frequency varies, the complex pressure amplitude changes in two main ways. 1) The amplitude decreases globally as the frequency increases. The 1000 Hz amplitude is so low compared to 200 Hz for the sawtooth source condition because it is the 10^{th} harmonic of the fundamental. Figure 24 (a) through (c) show the decay of the sawtooth signal at higher frequencies. 2) The source becomes more directional,

and is more characteristic of discrete sources than of a finite line source. The sawtooth source condition, Figure 24 (a) through (c), shows independent sources and the lobed spreading pattern from their interference. Parts (d) through (f) show the partially correlated source condition decreasing amplitude with increasing frequency and becoming more closely grouped around individual sources.

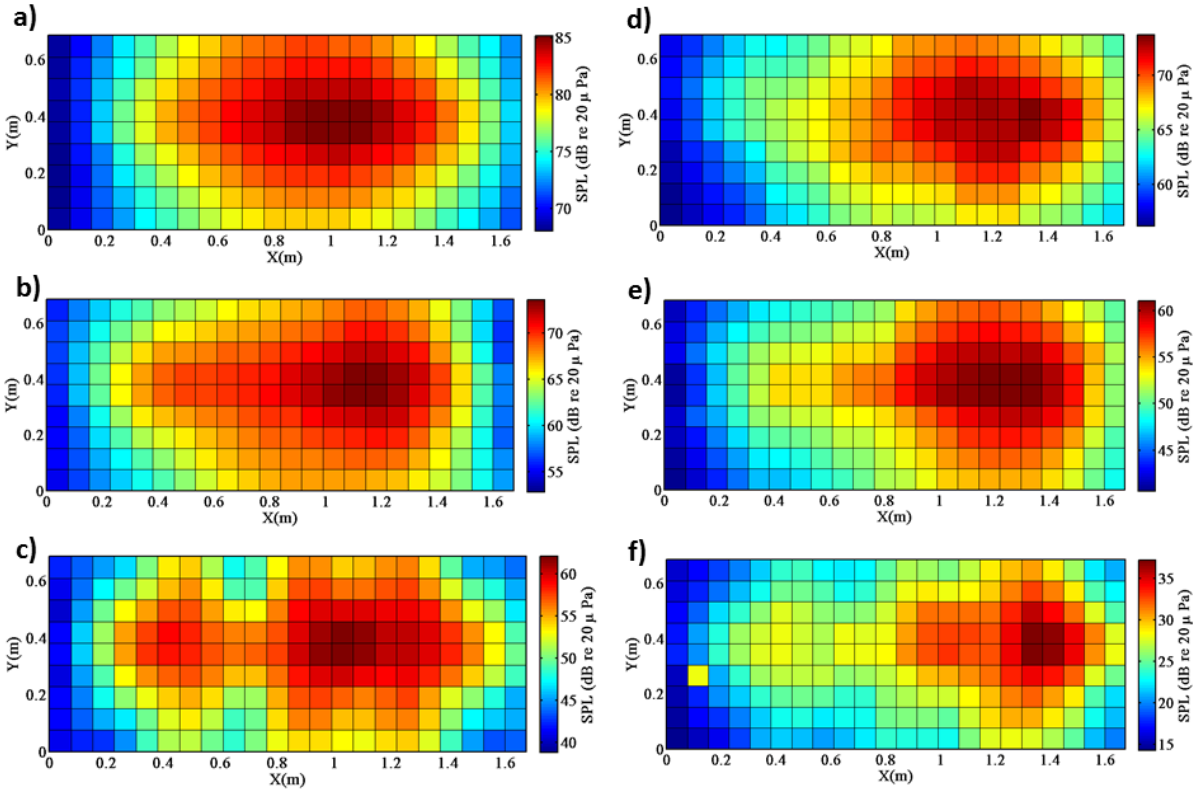

Figure 24: Plots showing how complex pressure amplitude of a line source varies with frequency. On the left, plots(a) through (c) show the sawtooth source condition measured at 200 Hz, 500 Hz, and 1000 Hz for plots a), b), and c) respectively. On the right, plots (d) through (f) show the partially correlated source condition measured at 200 Hz, 500 Hz, and 1000 Hz for plots (d), (e), and (f) respectively. All plots represent the 6" plane.

Each scan contains greater phase variation for higher frequencies. Figure 25 shows this phase variation changing from a fraction of a radian per scan at 200 Hz to about π radians per scan at 1000 Hz. If, with increasing frequency, the phase variation between measurement positions becomes greater than π, the algorithm will fail to unwrap, as this is the spatial Nyquist frequency. For the 3" microphone spacing used in this experiment, the spatial Nyquist frequency is 2250 Hz. Therefore, for all frequencies presented in Figure 25, the stitching algorithm will be effective. Phase variation across individual scans is a primary limiting factor of the 2-D unwrapping process (see section **Error! Reference source not ound.** for more details). This impact is another reason that frequency largely dictates whether creating a coherent plane of complex pressures and thereby performing NAH is possible.

Laboratory Experiment

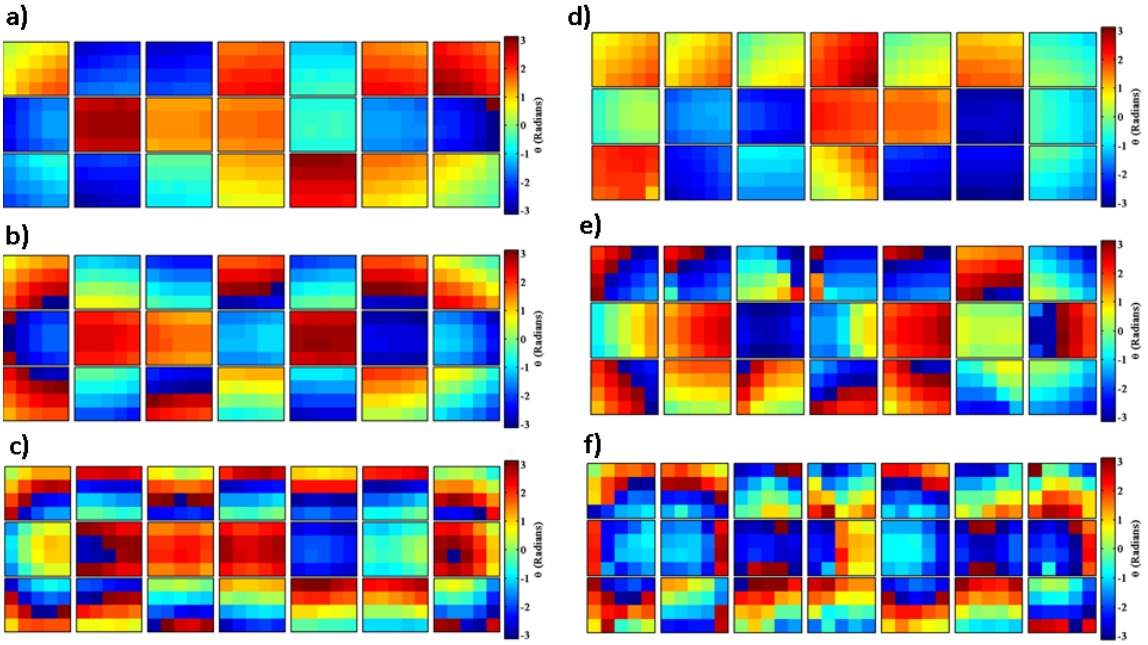

Figure 25: Plots showing how individual scans phase vary with frequency. On the left, plots(a) through (c) show the sawtooth source condition measured at 200 Hz, 500 Hz, and 1000 Hz for plots a), b), and c) respectively. On the right, plots (d) through (f) show the partially correlated source condition measured at 200 Hz, 500 Hz, and 1000 Hz for plots (d), (e), and (f) respectively. Planes of data for both source conditions were measured 6" from the source. The phase variation across a single scan increases with frequency because of the shortening wavelength.

The increased source directionality seen via stitched complex pressure amplitude in Figure 24 can also be seen by the stitched complex pressure phase. At low frequencies, the entire line source is in phase, and radiates as a cylinder (Figure 26a). At high frequencies, the phase pattern reveals the individual sources composing the line source (Figure 26c).

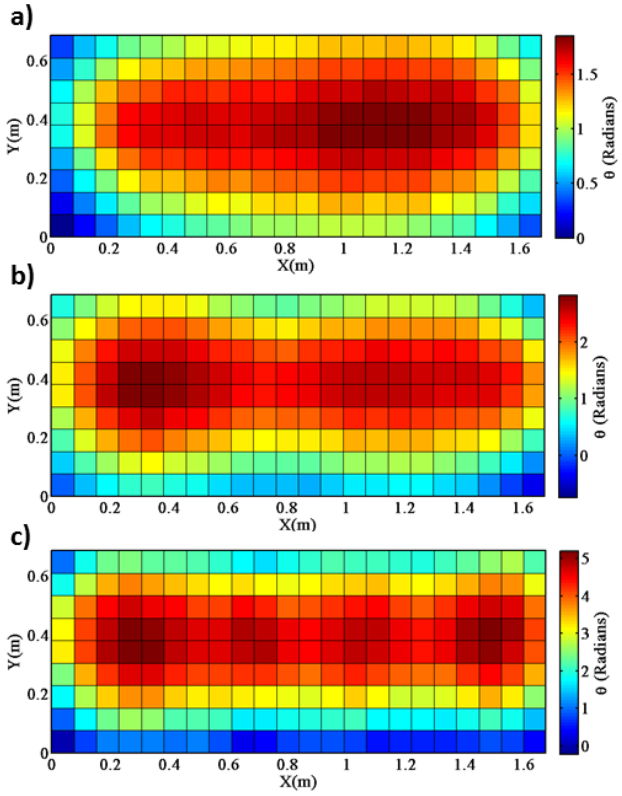

Figure 26: Plots showing how stitched phase varies with frequency. (a), (b), and (c) show stitched and averaged phase for the sawtooth source condition measured at 6" for 200 Hz, 500Hz, and 1000 Hz respectively. The source resolution increases with frequency because the distance between sources relative to a wavelength increases.

3.4.3 Height Comparison

In this experiment, two parallel planes of data were taken at 1" and 6" from the source (see Figure 9 and Figure 10 of section 3.1). The 6" plane is far enough from the source to perform NAH. The 1" plane provides a useful benchmark to assess the effectiveness of using NAH to project the 6" data to 1". A comparison of the complex pressure amplitudes of the sawtooth source condition measured at 1" and at 6" is shown in Figure 27. The 1" plane of data directly shows the source location, shape, and amplitude. When the source is measured at 6", the amplitude has decayed significantly because of geometric spreading, the fields from individual sources are superimposed, and the source shape is no longer clearly distinguishable.

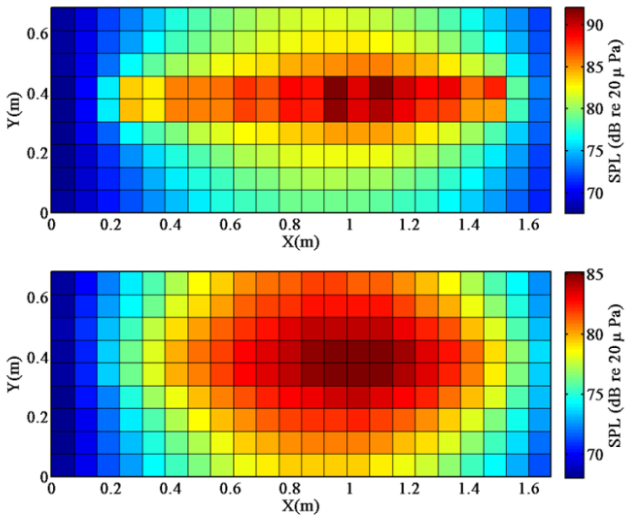

Figure 27: Plots showing how stitched amplitude varies with height. Both plots show the stitched amplitude of the sawtooth source condition at 200 Hz. Data for the top plot was collected with the scanning rig positioned 1" above the source, and data for the bottom plot was collected with the scanning rig positioned 6" above the source.

The difference between the two plots in Figure 27 nicely illustrates the necessity of NAH. Holography, when properly performed, can take data measured at a distance from the source which fails to show a fine resolution of source shape and amplitude and produce the data as if it were measured at a close distance. For jet noise where taking measurements a 1" is impossible, this is a crucial tool in gaining a finely resolved picture of what "jet noise" actually looks like.

3.5 Validation

If the results presented above are valid, they will suggest the ability of this stitching technique to create a coherent measurement plane using only the relationship between overlapping regions in scan-by-scan measurements. This ability can be validated by comparing the local coherence across the measurement plane before and after the method is applied. If the local coherence is preserved while global coherence is calculated across the plane, then the method will be considered a success.

To test this validation requirement, the local coherence between two microphones on each scan in a horizontal line of adjacent scans was calculated before and after the scans were stitched together. The microphones used before stitching are pictured in the top schematic in Figure 28. This figure shows two microphones in the same place in the measurement array, when the array was moved to the seven center scan positions. After the entire measurement plane's amplitude was stitched and phase was unwrapped and stitched, the coherence between the resulting complex pressures at every consecutive measurement position in one row was calculated. Comparing these, now continuous, results to those from the original complex pressures will show if the local coherence was preserved during the unwrapping and stitching process.

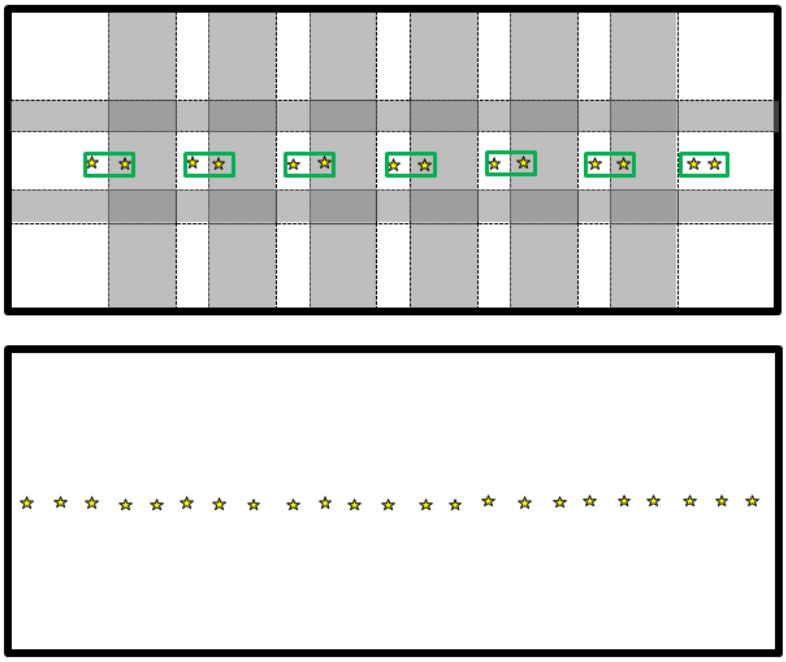

Figure 28: Diagram representing where local coherence was checked before and after stitching and unwrapping to validate effectiveness of the method. The top schematic shows pairs of microphones used in each of 7 adjacent horizontal scans to calculate local coherence before stitching and unwrapping shown in Figure 29 A) and B). The bottom schematic shows a row of microphones in the unwrapped and stitched array. Local coherence was calculated between each pair of adjacent microphones and is shown in Figure 29 C) and D).

The results of this analysis are shown in Figure 29. The local coherence for the center microphones in each of 7 adjacent horizontal scans pictured in the top schematic of Figure 28 are shown in Figure 29 a) and b) for partially coherent white noise and incoherent white noise respectively. The continuous coherence for this same row of data – now stitched – is shown in c) and d) of Figure 29. These results show that the stitching method preserves the consistently high local coherence between measurement positions, while temporally correlating the entire scan.

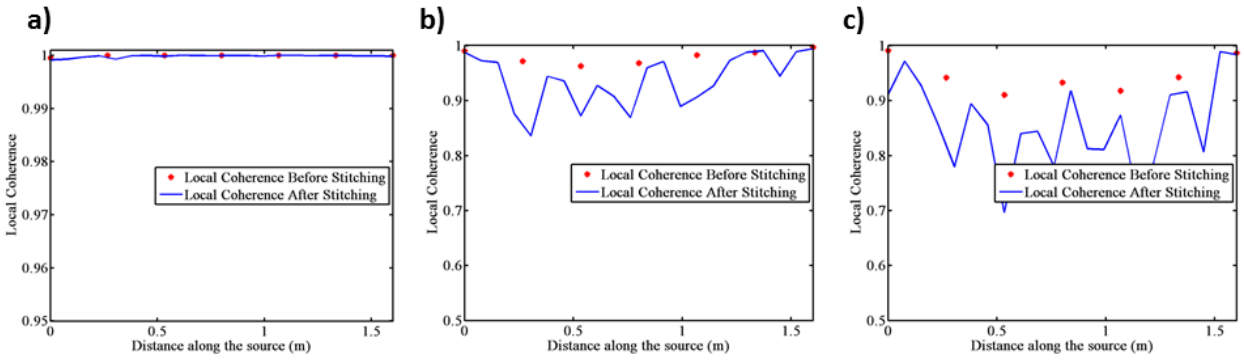

Figure 29: Plots showing the effect of stitching and unwrapping on local coherence. The red dots indicate coherence between two microphones on the array at each of 7 horizontal positions before the scans' phase and amplitude are unwrapped and stitched. The blue lines show local coherence between each pair of adjacent microphones moving across the fully stitched array on one horizontal row of 23 microphone positions, representing the now continuous phase. A) is for the correlated white noise source, B) is for the partially correlated condition, and C) is for the uncorrelated source condition. Note that the local coherence is not significantly diminished by the unwrapping and stitching process.

Chapter 4: Full Scale Jet Experiment

4.1 Measurements

Acoustic measurements of an F-22 Raptor jet engine were taken in July of 2009 at Holloman Air Force Base. The F-22 is a dual-engine tactical aircraft. For this test, the aircraft was secured to an open-air concrete run-up facility and one engine was operated at four engine conditions: idle, intermediate, military, and afterburner. The aircraft operating at afterburner condition on the concrete run-up pad is pictured in Figure 30. Full details about the experiment can be read in the referenced paper by Wall et al.[16]

Figure 30: F-22 Raptor tethered to the run-up pad. The 90-microphone array is shown on the track that allowed it to move in 2.3 m increments horizontally, parallel to the shear layer, and 0.6 m increments vertically.

Data acquired in this experiment were collected by free-field pressure microphones arranged on a 5 x 15 microphone rig that was moved to 30 positions to create a plane of measurements parallel to the jet plume. All rig positions are represented by red triangles in Figure 31, but only the plane surrounded by the green rectangle will be considered here. Including the overlapped regions, the final measurement array size was 1.8 x 22.9 m. Specifics about the rig, overlap, and microphones are detailed in a paper by Morgan et al.[17]

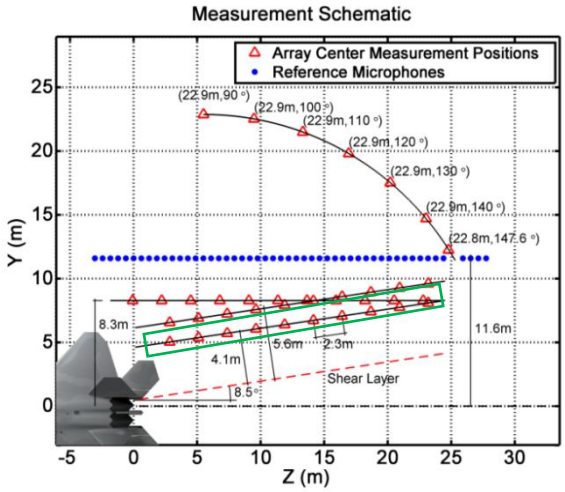

Figure 31: Measurement Schematic of the acoustical measurements of an F-22 Raptor. The red triangles indicate the center of a 90-microphone array for individual scan positions. At each scan position there were three measurement positions vertically. The green rectangle indicates the plane of data analyzed in this paper. The blue dots mark 50 stationary reference microphones traditionally used for stitching together the scans for use in NAH.

Military aircraft noise presents a turbulent extended source far more complicated than the laboratory source. One difference between the experiments is the presence of ground reflections in the full-scale outdoor test. These ground reflections introduce a problematic physical 180° phase shift in the data that will negatively impact the possibility of phase unwrapping (discussed further in section 2.1.1). This limits the frequency range that the self-referencing stitching algorithm can be applied to.

Another important difference between the lab test and the full-scale experiment is the source. Supersonic jet noise contains nonlinearity not present in the lab source. Additionally, while jet noise is partially correlated, the correlated and uncorrelated components are not simple like the lab source described in section 3.2. Despite these major differences, jet noise can still be modeled as a partially correlated line array of simple sources.[17 18] This allows treatment of a full-scale jet experiment as an expansion of the laboratory experiment.

The stitching and unwrapping technique described in Chapter 2 has been preliminarily applied to jet noise in much the same way as it was applied to lab-data in chapter 3.4.1 . Complex pressure amplitudes for the entire plane of data represented by the green triangle in Figure 31 were stitched together while maintaining the total energy across the entire scan using the method described in section 2.2.2. Then the complex pressure phases were unwrapped and stitched together. A preview of these results is given below.

4.2 Results

Figure 32 shows single block phase stitching results for different frequencies. Frequencies pictured are 80 Hz, 125 Hz (near the peak frequency of jet noise), 315 Hz, and 500 Hz. The legend for each plot is different because for high frequencies, the 1.8 x 22.9 m array spans many periods. There are some phase discontinuities present in the data, but this is only a single block representation, and is smoothed in the ensemble averaging process (see Figure 19 for the analog plot made using the lab experiment data). The stitched phase plot has fewer discontinuities in the downstream region where the source is more coherent.

Full Scale Jet Experiment

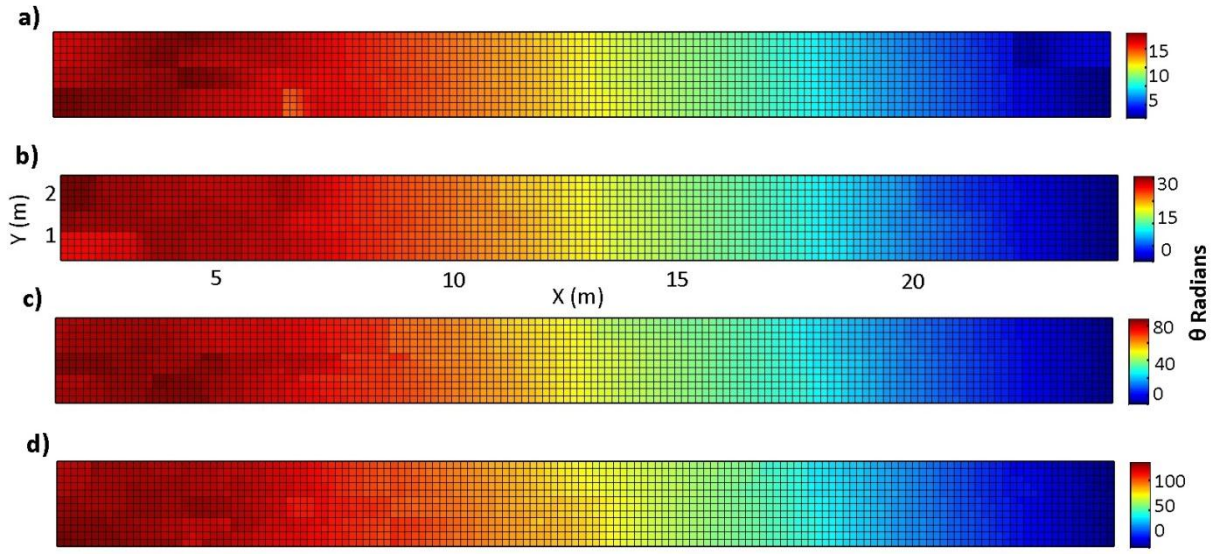

Figure 32: One block of stitched phase of complex pressure plane taken from the F-22 operating at military condition analyzed at several frequencies: A) 80 Hz, B) 125 Hz, B) 315 Hz, and D) 500 Hz. Upstream turbulence exceeds downstream turbulence. Phase variation over the array varies greatly between a) and d).

For frequencies up to 500 Hz, the stitching algorithm works well. Above 500 Hz, interference nulls due to ground reflections create a phase shift in the measurement plane that impedes unwrapping efforts. Additionally, at high frequencies the local coherence decreases, and the spatial Nyquist frequency is approached.

Chapter 5: Conclusions

5.1 Summary of Present Work

In this thesis, a novel technique of creating a coherent complex pressure array was presented. This method uses the local coherence between measurement positions in regions of spatial overlap between scan-based measurements to stitch together phase and amplitude. The resulting complex pressure plane is temporally correlated and can be used for future phase-based analysis such as NAH.

The technique presented here has two major steps: 1) unwrapping, and 2) stitching. Two-dimensional phase unwrapping of individual scans was performed and phase stitching was achieved, while maintaining the intra-scan phase relationships, by extracting the phase differences between scans from the overlapping measurement regions. Amplitude stitching was achieved while maintaining the total energy across the scan. This technique was validated using laboratory experimental data and then applied to jet noise data. An experiment measuring a line source with overlapping scan-based measurements was designed to validate the technique and is detailed here. The method was applied to this experimental data at various source conditions and the results have been presented. The technique's validity was confirmed using coherence analysis. Preliminary results of this technique applied to jet noise were shown in Chapter 4. While jet noise is a significantly more complex source than a line array of speakers, the stitching technique is still effective because of the local coherence provided by the partially correlated source.

5.2 Suggestions for Future Work

This work is a precursor to make performing NAH on large-scale measurements more experimentally and computationally efficient. Therefore, the steps following this project naturally include performing NAH on complex pressures processed using this technique. The following are suggested steps for expanding this method for future use.

1) Create a coherent complex pressure plane using the stationary reference microphones. Compare the resulting amplitude and phases obtained from this traditional method to those obtained using the new method for all source conditions of the experimental data.
2) Perform NAH on the 6" plane of experimental data to recreate the conditions at 1" away from the source. Compare this reproduction with the measured pressures at 1".
3) Apply the technique to jet noise data and then perform NAH to infer source conditions.

Chapter 6 References

[1] M. J. Lighthill, "On sound generated aerodynamically. II. Turbulence as a source of sound," Royal Society of London. Series A, Mathematical and Physical Sciences **222**, 1-32 (1954).

[2] K. Viswanathan, "Mechanisms of jet noise generation: Classical theories and recent developments", Int. J. of Aeroacoustics,8, 355–407, (2009).

[3] C. K. W. Tam, K. Viswanathan, K. K. Ahuja and J. Panda, "The sources of jet noise: Experimental evidence," J. Fluid Mech. **615**, 253-292 (2008).

[4] C.K.W. Tam, M. Golebiowski and J.M. Seiner, "On the Two Components of Turbulent Mixing Noise from Supersonic Jets", AIAA paper 96-1716, (1996).

[5] M. Lee, J. S. Bolton, "Source characterization of a subsonic jet by using near-field acoustical holography," J. Acoust. Soc. Am. **121**, 967-977 (2007).

[6] A.F. Metherell, H.M. El-Sum, J.J. Dreher, and L. Larmore, "Introduction to acoustical holography," J. Acoust. Soc. Am. **42**, 733 (1967).

[7] Y.T. Cho, J.S. Bolton, and J. Hald, "Source visualization by using statistically optimized near-field acoustical holography in cylindrical coordinates," J. Acoust. Soc. Am. **118**, 2355 (2005).

[8] E. G. Williams, *Fourier acoustics: Sound radiation and nearfield acoustical holography* (Academic Press, San Diego, 1999).

[9] A. T. Wall, *The Characterization of Military Aircraft Jet Noise Using Near-Field Acoustical Holography Methods* (Ph.D. dissertation, Brigham Young University, Provo, UT, 2013).

[10] A.T. Wall, K.L. Gee, M.D. Gardner, T.B. Neilsen and M.M. James, "Near-field acoustical holography applied to high-performance jet aircraft noise", Mtgs. Acoust., 9, 040009, (2011).

[11] J. D. Maynard, E. G. Williams, and Y. Lee, "Nearfield acoustic holography: I. Theory of generalized holography and the development of NAH," J. Acoust. Soc. Am. 78 (4) 1395-1413 (1985).

[12] M. Lee and J. S. Bolton, "Scan-based near-field acoustical holography and partial field decomposition in the presence of noise and source level variation," J. Acoust. Soc. Am. **119**, 382-393 (2006).

[13] D. Ghiglia and M. Pritt Two-dimensional phase unwrapping theory, algorithms and software, John Wiley & Sons, 1998.

[14] M. Gdeisat and F. Lilley, "Two-Dimensional Phase Unwrapping Problem,"

[15] M. Arevalillo Herráez, D. R. Burton, M. J. Lalor and M. A. Gdeisat, "A Fast two-dimensional phase unwrapping algorithm based on sorting by reliability following a non-continuous path," Applied Optics, Vol. 41, No. 35, pp 7437-7444, 2002.

[16] A.T. Wall, K.L. Gee, M.M. James, K.A. Bradley, S.A. McInerny and T.B. Neilsen, "Near-field noise measurements of a high-performance military jet aircraft", Noise Control Engr. J. **60**, 421–434, (2012).

[17] J. Morgan, T.B. Neilsen, K.L. Gee, A.T. Wall, M.M. James, "Simple-source model of military jet aircraft noise," Noise Control Engr. J. **60**, 435-449 (2012).

[18] D. M. Hart, T. B. Neilsen, K. L. Gee and M. M. James, "A Bayesian based equivalent sound source model for a military jet aircraft," Proceedings of 21st International Congress on Acoustics, 2012.

Appendix 1:

Stitching and Unwrapping Algorithm

This algorithm reads in time-waveform pressure values from the data acquisition software. The time waveform is processed to remove the DC offset. The number of samples per time block is selected, and then the single-sided Fourier transform is taken of the time waveform. This yields complex pressures for each frequency block. From this point, the complex pressure phases of individual measurement scans are unwrapped. Then the phases and amplitudes are stitched together. The last line combines the stitched phase and amplitude into CP, the final complex pressure array.

```
% Process Data and save CP (complex pressure) matricies
% 4/12/2014

clear all;
close all;

% INPUT PARAMETERS
% Define Source
S = 2;  % 1 = correlated, 2 = partial, 3 = uncorrelated, 4 = sawtooth
H = 2;  % define height. 1 = 1", 2 = 6"
fint =165; % frequency index of interest to save (165 is 1000 Hz, 34 is 200
Hz, 43 is 250 Hz, 83 is 500 Hz)
F = 1000;
% Define Test. 2 = 1 in,  3 = 6 in, 4 = 6 in broadband
pathname='S:\Students\Blaine
Harker\Phase_Stitch_Experiment\Data\Data_20140127\';
testname=(['Phase_Stiching_Test2_H',num2str(H),'_S',num2str(S)']);

fs=50000; % Sampling Frequency
ns = 2^13; % Number of Samples per block
f = fs*(0:ns/2-1)/ns; % freq. scale for ss fft.;
df = f(2) - f(1);% width of frequency bins
ww = hann(ns); % generates the window.  .' is used to get the right
orientation.
W = mean(ww.*conj(ww)); % used to scale the psd
Xss= zeros(20,21,15); % Initialize complex pressure
Gxx = zeros(20,21); % Initialize PSD
freq = f(fint);

% LOAD DATA AND SAVE COMPLEX PRESSURE

for ID = 1:21 % Scan Position Number
    for CH = 1:20 % Channel Number

        % Read in waveform
```

```
filename=[pathname,testname,'_',sprintf('%03i',ID),'_',sprintf('%03i',CH-
1),'.bin'];
        fid = fopen(filename,'r');
        x = fread(fid,inf,'single');
        fclose(fid);

        x = x - mean(x); % Remove any DC offset
        N = length(x); % Length of File
        t = (0:N-1)/fs; % Time Vector

        % Calculate the Complex Pressures:
        N = 2^floor(log2(length(x)));
        x = x(1:N); % makes length a power of 2
        blocks = zeros(2*N/ns-1,ns);
        blocks(1,:) = ww.*x(1:ns);

        for kk = 2:2*N/ns-1;
            blocks(kk,:) = ww.*x((kk-1)*ns/2:(kk+1)*ns/2-1);
        end

        X = sqrt(2*df/ns/fs/W)*fft(blocks,ns,2);
        Gxx(CH,ID) = mean(X(:, fint).*conj(X(:,fint)));
        Xss(CH,ID,:) = X(:,fint); % Single Sided Complex Pressure
    end
end

% FORMAT COMPLEX PRESSURE MATRICIES TO MATCH TEST SHAPE

cp = reshape(Xss,5,4,7,3,15);
cp = permute(cp, [1 2 4 3 5]);

gp = reshape(Gxx,5,4,7,3);
gp = permute(gp, [1 2 4 3]);

% COMPLETE STITCHING AND UNWRAPPING METHOD

% AVERAGE AND STITCH AMPLITUDE
mag = mean(abs(cp(:,:,:,:,:)).^2,5); % calculate the average amplitude for
each position across all blocks

% Arrange matrix to array size
magCall = vertcat(mag(:,:,2,1), mag(3:5,:,2,2), mag(3:5,:,2,3),
mag(3:5,:,2,4),mag(3:5,:,2,5),mag(3:5,:,2,6),mag(3:5,:,2,7));
magTall = vertcat(mag(:,:,3,1), mag(3:5,:,3,2), mag(3:5,:,3,3),
mag(3:5,:,3,4),mag(3:5,:,3,5),mag(3:5,:,3,6),mag(3:5,:,3,7));
magBall = vertcat(mag(:,:,1,1), mag(3:5,:,1,2), mag(3:5,:,1,3),
mag(3:5,:,1,4),mag(3:5,:,1,5),mag(3:5,:,1,6),mag(3:5,:,1,7));

magall = horzcat(magTall, magCall(:, 2:3), magBall); % array of averaged and
stitched amplitudes

% UNWRAP AND STITCH PHASE
```

References

```
for blk = 1:63
    % UNWRAP PHASE - using unwrapping algorithm available at
http://www.ljmu.ac.uk/GERI/90223.htm
    load(['cp_S',num2str(S),'_H',num2str(H),'_',num2str(F),'Hz.mat'])
    cp = cp(:,:,:,:,blk);

    thC = zeros(5,4,7); % thC is the center row
    for n=1:7
        thC(:,:,n) = Miguel_2D_unwrapper(single(angle(cp(:,:,2,n))));
    end

    thT = zeros(5,4,7); % thT is the top row
    for n=1:7
        thT(:,:,n) = Miguel_2D_unwrapper(single(angle(cp(:,:,3,n))));
    end

    thB = zeros(5,4,7); % thB is the bottom row
    for n=1:7
        thB(:,:,n) = Miguel_2D_unwrapper(single(angle(cp(:,:,1,n))));
    end

    % STITCH PHASE

    % stitch phase for the first three scans from the right
    % calculate first shifts, average of all overlapping microphone
differences.
    Dth2 = median(median(thC(4:5,:,6)-thC(1:2,:,7))); % Left Bound
    DthT1 = median(median(thT(:,4,7)-thC(:,1,7))); % Center to Top
    DthB1 = median(median(thB(:,1,7)-thC(:,4,7))); % Center to Bottom

    % apply shifts to Top, center second, and Bottom scans
    thC(:,:,6) = thC(:,:,6) - Dth2;
    thT(:,:,7) = thT(:,:,7) - DthT1;
    thB(:,:,7) = thB(:,:,7) - DthB1;

    % Initialize difference matricies
    ADthT = zeros(3,6); % Average Delta Theta Top
    DthT = zeros(7,1); % Delta Theta Top
    ADthB = zeros(3,6); % Average Delta Theta Bottom
    DthB = zeros(7,1); % Delta Theta Bottom
    ADthC = zeros(3,6); % Average Delta Theta Center
    DthC = zeros(7,1); % Delta Theta Center

    % STITCH TOGETHER USING COMPREHENSIVE ALGORITHM
    for n = [6 5 4 3 2]

        % Calculate top shift
        % top -> top (straight across)
        DthT1T2 = median(median(thT(4:5,:,n) - thT(1:2,:,n+1)));
        % center -> top (diagonally up)
        DthC1T2 = median(median(thT(4:5,4,n) - thC(1:2,1,n+1)));
        % center -> top (straight up)
        DthC2T2 = median(median(thT(:,4,n) - thC(:,1,n)));
        % Top averaqge
```

```
        ADthT(:,n) = [DthT1T2 DthC1T2 DthC2T2];
        DthT(n) = median(ADthT(:,n));

        % Apply average to next top scan
        thT(:,:,n) = thT(:,:,n) - DthT(n);

        % Calculate bottm scan
        % bottom -> bottom (straight across)
        DthB1B2 = median(median(thB(4:5,:,n) - thB(1:2,:,n+1)));
        % center -> botom (diagonally down)
        DthC1B2 = median(median(thB(4:5,1,n) - thC(1:2,4,n+1)));
        % center -> bottom (straight down)
        DthC2B2 = median(median(thB(:,1,n) - thC(:,4,n)));
        % Bottom average
        ADthB(:,n) = [DthB1B2 DthC1B2 DthC2B2];
        DthB(n) = median(ADthB(:,n));

        % Apply average to next bottom scan
        thB(:,:,n) = thB(:,:,n) - DthB(n);

        % Calculate next center shift (n-1)
        % center -> center (straight across)
        DthC1C2 = median(median(thC(4:5,:,n-1) - thC(1:2,:,n)));
        % top -> center (diagonally down)
        DthT1C2 = median(median(thC(4:5,1,n-1) - thT(1:2,4,n)));
        % bottom -> center (diagonally up)
        DthB1C2 = median(median(thC(4:5,4,n-1) - thB(1:2,1,n)));
        % Center average
        ADthC(:,n) = [DthC1C2 DthT1C2 DthB1C2];
        DthC(n) = median(ADthC(:,n));

        % Apply average to next center scan
        thC(:,:,n-1) = thC(:,:,n-1) - DthC(n);

    end

    % calculate final shift for top and bottom scan on far left
    % Calculate top shift
    % top -> top (straight across)
    DthT1T2 = median(median(thT(4:5,:,1) - thT(1:2,:,2)));
    % center -> top (diagonally up)
    DthC1T2 = median(median(thT(4:5,4,1) - thC(1:2,1,2)));
    % center -> top (straight up)
    DthC2T2 = median(median(thT(:,4,1) - thC(:,1,1)));
    % top average
    ADthT(:,1) = [DthT1T2 DthC1T2 DthC2T2];
    DthT(1) = median(ADthT(:,1));

    % Apply average to next top scan
    thT(:,:,1) = thT(:,:,1) - DthT(1);

    % Calculate bottom shift
    % bottom -> bottom (straight across)
    DthB1B2 = median(median(thB(4:5,:,1) - thB(1:2,:,2)));
```

```
    % center -> botom (diagonally down)
    DthC1B2 = median(median(thB(4:5,1,1) - thC(1:2,4,2)));
    % center -> bottom (straight down)
    DthC2B2 = median(median(thB(:,1,1) - thC(:,4,1)));
    % Bottom average
    ADthB(:,1) = [DthB1B2 DthC1B2 DthC2B2];
    DthB(1) = median(ADthB(:,1));

    % Apply average to next bottom scan
    thB(:,:,1) = thB(:,:,1) - DthB(1);

    % Reshape matrix to size of array
    thCall = vertcat(thC(:,:,1), thC(3:5,:,2), thC(3:5,:,3), thC(3:5,:,4),
thC(3:5,:,5), thC(3:5,:,6), thC(3:5,:,7));
    thTall = vertcat(thT(:,:,1), thT(3:5,:,2), thT(3:5,:,3), thT(3:5,:,4),
thT(3:5,:,5), thT(3:5,:,6), thT(3:5,:,7));
    thBall = vertcat(thB(:,:,1), thB(3:5,:,2), thB(3:5,:,3), thB(3:5,:,4),
thB(3:5,:,5), thB(3:5,:,6), thB(3:5,:,7));
    theta(:,:,blk)  = horzcat(thTall, thCall(:, 2:3), thBall);
end

% Zero out each block and ensemble average
for blk = 1:63
    theta(:,:,blk) = theta(:,:,blk) - theta(1,1,blk);
end
thetaavg = mean(theta, 3);

% Create stitched complex pressure
CP = magall.* exp(1i.*thetaavg);
```